Inorg. Chem. **2007**, *46*, 4336–4356

1,4,7,10-Tetraazacyclododecane Metal Complexes as Potent Promoters of Carboxyester Hydrolysis under Physiological Conditions

Michael Subat, Kristina Woinaroschy, Stefan Anthofer, Barbara Malterer, and Burkhard König*

Institute for Organic Chemistry, University of Regensburg, Universitätsstrasse 31, D-93053 Regensburg, Germany

Received January 19, 2007

New 1,4,7,10-tetrazacyclododecane ([12]aneN$_4$ or cyclen) ligands with different heterocyclic spacers (triazine and pyridine) of various lengths (bi- and tripyridine) or an azacrown pendant and their mono- and dinuclear Zn(II), Cu(II), and Ni(II) complexes have been synthesized and characterized. The pK_a values of water molecules coordinated to the complexed metal ions were determined by potentiometric pH titrations and vary from 7.7 to 11.2, depending on the metal-ion and ligand properties. The X-ray structure of [**Zn$_2$L2**]μ-OH(ClO$_4$)$_3$·CH$_3$CN·H$_2$O shows each Zn(II) ion in a tetrahedral geometry, binding to three N atoms of cyclen (the average distance of Zn–N = 2.1 Å) and having a μ-OH bridge at the apical site linking the two metal ions (the average distance of Zn–O$^-$ = 1.9 Å). The distance between the Zn(II) ion and the fourth N atom is 2.6 Å. All Zn(II) complexes promote the hydrolysis of 4-nitrophenyl acetate (NA) under physiological conditions, while those of Cu(II) and Ni(II) do not have a significant effect on the hydrolysis reaction. The kinetic studies in buffered solutions (0.05 M Tris, HEPES, or CHES, I = 0.1 M, NaCl) at 25 °C in the pH range of 6–11 under pseudo-first-order reaction conditions (excess of the metal complex) were analyzed by applying the method of initial rates. Comparison of the second-order pH-independent rate constants (k_{NA}, M^{-1} s^{-1}) for the mononuclear complexes **ZnL1**, **ZnL3**, and **ZnL8**, which are 0.39, 0.27, and 0.38, respectively, indicates that the heterocyclic moiety improves the rate of hydrolysis up to 4 times over the parent Zn([12]aneN$_4$) complex (k_{NA} = 0.09 M^{-1} s^{-1}). The reactive species is the Zn(II)–OH$^-$ complex, in which the Zn(II)-bound OH$^-$ acts as a nucleophile, which attacks intermolecularly the carbonyl group of the acetate ester. For dinuclear complexes **Zn$_2$L2**, **Zn$_2$L4**, **Zn$_2$L5**, **Zn$_2$L6**, and **Zn$_2$L7**, the mechanism of the reaction is defined by the degree of cooperation between the metal centers, determined by the spacer length. For **Zn$_2$L7**, having the longest triaryl spacer, the two metal centers act independently in the hydrolysis; therefore, the reaction rate is twice as high as the rate of the mononuclear analogue (k_{NA} = 0.78 M^{-1} s^{-1}). The complexes with a monoaryl spacer show saturation kinetics with the formation of a Michaelis–Menten adduct. Their hydrolysis rates are 40 times higher than that of the Zn[12]aneN$_4$ system ($k_{NA} \sim$ 4 M^{-1} s^{-1}). **Zn$_2$L6** is a hybrid between these two mechanisms; a clear saturation curve is not visible nor are the metal cores completely independent from one another. Some of the Zn(II) complexes show a higher hydrolytic activity under physiological conditions compared to other previously reported complexes of this type.

Introduction

Hydrolytic enzymes often use water molecules or protein hydroxy residues (e.g., of serine or threonine) as nucleophiles to react with electrophilic substrates (carboxyesters, phosphate esters, and amides), wherein the prior activation of the nucleophiles (and/or electrophiles) is essential.[1] These enzymes often require metal cations for their activity,[2] and many metal-ion-based model systems have been reported, generally featuring tridentate or tetradentate ligands with free coordination sites on the metal cation.[3] Polyamine macro-

* To whom correspondence should be addressed. E-mail: burkhard.koenig@chemie.uni-regensburg.de.

(1) (a) Neuberger, A.; Brocklehurst, K. *Hydrolytic Enzymes*; Elsevier Science: Amsterdam, The Netherlands, 1987. (b) Bertini, I.; Luchinat, C.; Maret, W.; Zeppesauer, M. *Zinc Enzymes*; Birkauser: Boston, 1986.

(2) For reviews on metallohydrolases, see: (a) Wilcox, D. E. *Chem. Rev.* **1996**, *96*, 2435. (b) Sträter, N.; Lipscomb, W. N.; Klabunde, T.; Krebs, B. *Angew. Chem., Int. Ed. Engl.* **1996**, *35*, 2024. (c) Lipscomb, W. N.; Sträter, N. *Chem. Rev.* **1996**, *96*, 2375.

10.1021/ic070101z CCC: $37.00
Published on Web 04/20/2007

Chart 1[a]

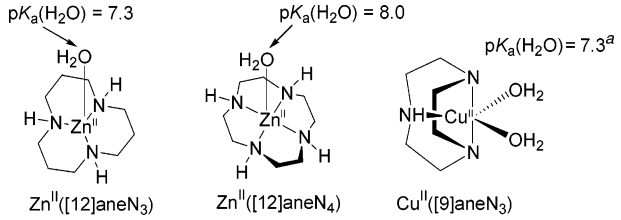

[a] Because of a monomer−dimer equilibrium, this pK_a is not simply the pK_a of the coordinated water; it is, however, the kinetically relevant pK_a.

cyclic ligands have received special attention in this respect. They are able to adapt to many metal-ion coordination geometries,[4] offer multiple donors sites, and are able to hold two metal ions at short distances, mimicking the active sites of metalloenzymes. The Zn(II) complexes of 1,5,9-triazacyclododecane ([12]aneN$_3$), 1,4,7,10-tetraazacyclododecane ([12]aneN$_4$) (Chart 1), and their derivatives have been suggested as chemical models of the active center of alkaline phosphatase,[5] carbonic anhydrase (CA),[6] carboxypeptidase,[7] liver alcohol dehydrogenase,[8] or β-lactamase.[9] Likewise, Cu(II) complexes of 1,4,7-triazacyclononane ([9]aneN$_3$; Chart 1) have been discussed as chemical models of phosphatases,[10] nucleases,[11] and peptidases.[12] The detoxification of some pesticides and chemical weapons was envisaged as a possible application of the compounds.[13]

The proposed general mechanism of the hydrolysis reaction promoted by these complexes is based on the Lewis acidic metal ion reducing the pK_a of the coordinated water, thus providing a metal-bound hydroxide nucleophile at neutral pH and at the same time activating the substrate toward nucleophilic attack by charge neutralization.[3a,14] For dinuclear species, the two metal ions act cooperatively in the catalytic process; either one metal ion provides the nucleophile and the other one coordinates the substrate or both metal ions participate in substrate binding, activation, and cleavage.[15] This cooperative action renders dinuclear complexes far more reactive than their mononuclear analogues.

Chart 2. Structures of the New [12]aneN$_4$ Ligands **L1**−**L8**

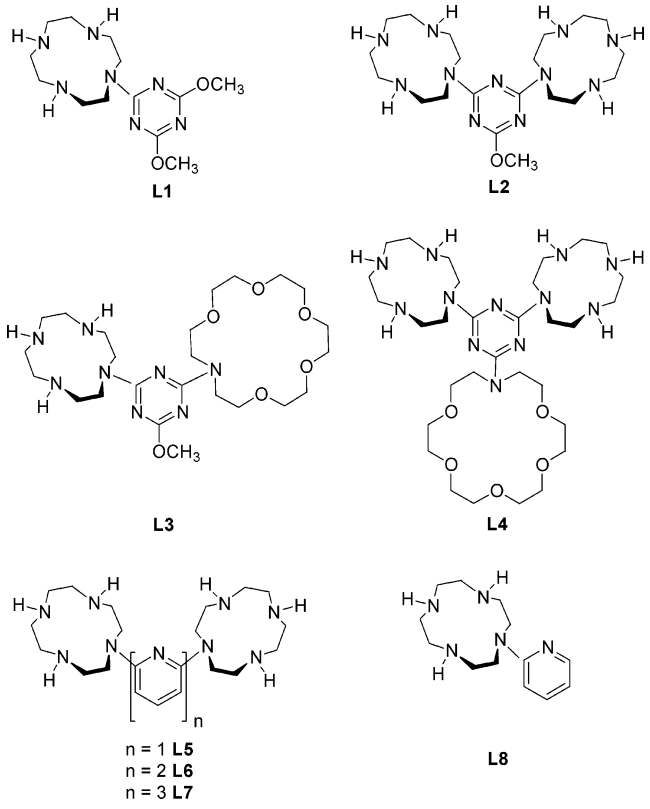

However, the hydrolytic activity of these synthetic systems with carboxyesters is moderate under physiological conditions. The second-order rate constants reach significant values only at pH values >9. Therefore, applications in biotechnology, medicine, or environmental sciences of the complexes would suffer from low efficiencies.

It has been demonstrated that additional interactions in the active site influence the properties of the metal complexes and that the hydrolytic activity may increase by attachment of functional groups to a chelate ligand,[16] such as a basic or nucleophilic auxiliary group[5b,17] or an NH acidic group.[18] With the aim to develop more efficient metal complexes possessing hydrolytic activity under physiological conditions, we have synthesized the macrocyclic ligands **L1**−**L8** (Chart 2) with different heterocyclic spacers of various lengths and

(3) For reviews, see: (a) Chin, J. *Acc. Chem. Res.* **1991**, *24*, 145. (b) Liu, C.; Wang, M.; Zhang, T.; Sun, H. *Coord. Chem. Rev.* **2004**, *248*, 147.
(4) For a review on thermodynamic and kinetic data for macrocycle interaction with cations, anions, and neutral molecules, see: Izatt, R. M.; Pawlak, K.; Bradshaw, J. S.; Bruening, R. L. *Chem. Rev.* **1995**, *95*, 2529.
(5) (a) Koike, T.; Kajitani, S.; Nakamura, I.; Kimura, E.; Shiro, M. *J. Am. Chem. Soc.* **1995**, *117*, 1210. (b) Kimura, E.; Kodama, Y.; Koike, T.; Shiro, M. *J. Am. Chem. Soc.* **1995**, *117*, 8304.
(6) Zhang, Z.; van Eldic, R.; Koike, T.; Kimura, E. *Inorg. Chem.* **1993**, *32*, 5749.
(7) Kim, D. H.; Lee, S. S. *Bioorg. Med. Chem.* **2000**, *8*, 647.
(8) Kimura, E.; Shionoya, M.; Hoshino, A.; Ikeda, T.; Yamada, Y. *J. Am. Chem. Soc.* **1992**, *114*, 10134.
(9) Koike, T.; Masahiro, M.; Kimura, E. *J. Am. Chem. Soc.* **1994**, *116*, 8443.
(10) (a) Belousoff, M. J.; Duriska, M. B.; Graham, B.; Batten, S. R.; Moubaraki, B.; Murray, K. S.; Spiccia, L. *Inorg. Chem.* **2006**, *45*, 3746. (b) Burstyn, J. N.; Deal, K. A. *Inorg. Chem.* **1993**, *32*, 3585. (c) Deal, K. A.; Burstyn, J. N. *Inorg. Chem.* **1996**, *35*, 2792.
(11) (a) McCue, K. P.; Voss, D. A., Jr.; Marks, C.; Morrow, J. R. *J. Chem. Soc., Dalton Trans.* **1998**, 2961. (b) Hegg, E. L.; Deal, K.; Kiessling, L.; Burstyn, J. N. *Inorg. Chem.* **1997**, *36*, 1715.
(12) Hegg, E. L.; Burstyn, J. N. *J. Am. Chem. Soc.* **1995**, *117*, 7015.
(13) Kimura, E.; Hashimoto, H.; Koike, T. *J. Am. Chem. Soc.* **1996**, *118*, 10963.
(14) (a) Hegg, E. L.; Burstyn, J. N. *Coord. Chem. Rev.* **1998**, *173*, 133. (b) Suh, J. *Acc. Chem. Res.* **1992**, *25*, 273.
(15) Göbel, M. W. *Angew. Chem., Int. Ed. Engl.* **1994**, *33*, 1141.
(16) (a) Kovbasyuk, L.; Krämer, R. *Chem. Rev.* **2004**, *104*, 3161. (b) Feng, G.; Mareque-Rivas, J. C.; de Rosales, R. T. M.; Williams, N. H. *J. Am. Chem. Soc.* **2005**, *127*, 13470. (c) O'Donoghue, A. M.; Pyun, S. Y.; Yang, M.-Y.; Morrow, J. R.; Richard, J. P. *J. Am. Chem. Soc.* **2006**, *128*, 1615.
(17) (a) Breslow, R.; Berger, D.; Huang, D.-L. *J. Am. Chem. Soc.* **1990**, *112*, 3686. (b) Morrow, J. R.; Aures, H.; Epstein, D. *J. Chem. Soc., Chem. Commun.* **1995**, 2431. (c) Young, M. J.; Wahnon, D.; Hynes, R. C.; Chin, J. *J. Am. Chem. Soc.* **1995**, *117*, 9441. (d) Chu, F.; Smith, J.; Lynch, V. M.; Anslyn, E. V. *Inorg. Chem.* **1995**, *34*, 5689 (the authors propose that in a Zn complex either imidazole or imidazolium might act as an auxiliary group, providing a 1.5-fold increase in the RNA cleavage rate). See also: (e) Hsu, C.-M.; Cooperman, B. S. *J. Am. Chem. Soc.* **1976**, *98*, 5657. (f) Koike, T.; Inoue, M.; Kimura, E.; Shiro, M. *J. Am. Chem. Soc.* **1996**, *118*, 3091.
(18) Kövari, E.; Krämer, R. *J. Am. Chem. Soc.* **1996**, *118*, 12704.

determined the hydrolytic properties of their Zn(II), Cu(II), and Ni(II) complexes in aqueous solution with 4-nitrophenyl acetate (NA). The influence of the following parameters on the hydrolytic efficiency and the mechanism of the hydrolysis reaction were analyzed: (i) metal complex spacer type and length; (ii) metal ion and its properties (synthesis of Cu(II) and Ni(II) complexes of **L1** and **L2**); (iii) number of metal ions present in the complex (comparison between mono- and dinuclear complexes).

Experimental Section

General Information. UV/vis spectra were recorded on a Varian Cary BIO 50 UV/vis/NIR spectrophotometer equipped with a jacketed cell holder using 1-cm cuvettes (quartz or glass) from Hellma and on a Zeiss SPECORD M500 spectrophotometer equipped with six cuvette holders using disposable acrylic [poly(methyl methacrylate)] 1-cm cuvettes from Sarstedt. For all UV/vis measurements, the temperature was kept constant at 25 °C (±0.1 °C). IR spectra were recorded on a Bio-Rad Fourier transform IR (FT-IR) FTS 155 spectrometer and a Bruker Tensor 27 spectrometer with an ATR unit. Elemental analysis was performed on a Vario EL III. Mass spectra were performed on a ThermoQuest Finnigan TSQ 7000 (ESI) and a Finnigan MAT 95 (high-resolution mass spectrometry, HRMS). Potentiometric titrations were performed with a Metrohm Dosimat 665. ^{1}H and ^{13}C NMR spectra were obtained on the following machines: Bruker AC-250 (^{1}H, 250.1 MHz; ^{13}C, 62.9 MHz; 24 °C), Bruker Avance 300 (^{1}H, 300.1 MHz; ^{13}C, 75.5 MHz; 27 °C), Bruker Avance 400 (^{1}H, 400.1 MHz; ^{13}C, 100.6 MHz; 27 °C), and Bruker Avance 600 (^{1}H, 600.1 MHz; ^{13}C, 150.1 MHz; 27 °C). Melting points were determined with a Büchi SMP 20 and are uncorrected.

Materials and Reagents. All reagents and solvents used for the synthesis of the metal complexes were of analytical grade. 4-Nitrophenyl acetate (NA; Fluka), 4-nitrophenol (4-NP; Riedel-de Haën), Tris (2-amino-2-hydroxymethyl-propane-1,3-diol; Usb), HEPES [*N*-(2-hydroxyethyl)piperazine-*N*′-(2-ethanesulfonic acid); Sigma], CHES (*N*-cyclohexyl-2-aminoethanesulfonic acid; Sigma), and acetonitrile [high-performance liquid chromatography (HPLC) grade; J.T. Baker] were purchased from commercial sources and used without any further purification. Cyclen was a generous gift from Schering and was used without further purification.

Caution! *Although no problems were encountered in this work, metal perchlorate complexes and perchloric acid are potentially explosive. They should be handled with care, and the complexes should be prepared in small quantities.*

Synthesis of Ligands and Metal Complexes. The synthetic intermediates 10-(4,6-dichloro-1,3,5-triazin-2-yl)-1,4,7,10-tetraazacyclododecane-1,4,7-tricarboxylic acid tri-*tert*-butyl ester (**1**),[19] 4,6-bis(1,4,7,10-tetraazacyclododecane-1,4,7-tricarboxylic acid tri-*tert*-butyl ester)-2-chloro-1,3,5-triazine (**4**),[20] 2,6-bis[1,4,7-tris(*tert*-butyloxycarbonyl)-1,4,7,10-tetraazacyclododecanyl]pyridine (**12**),[21] 6,6′-bis[1,4,7-tris(*tert*-butyloxycarbonyl)-1,4,7,10-tetraazacyclododecanyl]-2,2′-bipyridine (**14**),[21] and 10-(2-pyridinyl)-1,4,7,10-tetraazacyclododecane-1,4,7-tricarboxylic acid tri-*tert*-butyl ester (**18**)[21] were prepared according to published methods. Compound **16** was synthesized according to the published general procedure.[21]

10-(4,6-Dimethoxy-1,3,5-triazin-2-yl)-1,4,7,10-tetraazacyclododecane-1,4,7-tricarboxylic Acid Tri-*tert*-butyl Ester (2). A solution of **1**[19] (3.50 g, 5.65 mmol) in absolute methanol (25 mL) was treated under nitrogen with sodium methylate (0.85 g, 15.82 mmol), and the mixture was stirred for 18 h at room temperature. After completion of the reaction, the excess of NaOMe was quenched with a saturated aqueous solution of NH_4Cl (2 mL). The solvent was removed in vacuum, and the residue was purified by chromatography on silica (ethyl acetate/petroleum ether, 1:2) to give a colorless solid (R_f = 0.47, ethyl acetate/petroleum ether, 1:1): yield 3.38 g (98%); mp 70 °C; IR (KBr) $\tilde{\nu}$ [cm^{-1}] 2974, 2929, 1697, 1583, 1363, 1165, 679; UV/vis (CH_3CN) λ_{max} [nm] (log ϵ) 233 (4.489); ^{1}H NMR (400 MHz, $CDCl_3$) δ 1.37 (s, 18 H, CH_3−Boc), 1.43 (s, 9 H, CH_3−Boc), 3.34−3.53 (m, 8 H, CH_2−cyclen), 3.60 (bs, 4 H, CH_2−cyclen), 3.68 (bs, 4 H, CH_2−cyclen), 3.91 (s, 6 H, OCH_3); ^{13}C NMR (100 MHz, $CDCl_3$) δ 28.4, 28.5 (+, CH_3−Boc), 50.0, 50.3, 51.5 (−, CH_2−cyclen), 54.6 (+, OCH_3), 80.0, 80.3 (C_{quat}, C−Boc), 156.3, 157.1 (C_{quat}, C═O−Boc), 167.4 (C_{quat}, C_{aryl}−N), 171.9 (C_{quat}, C_{aryl}−OCH_3); MS (ESI, MeOH + 1% AcOH) *m*/*z* (%) 612 (100) [MH]$^+$, 634 (10) [M + Na]$^+$. Anal. Calcd for $C_{28}H_{49}N_7O_8$: C, 54.98; H, 8.07; N, 16.03. Found: C, 54.88; H, 8.02; N, 15.60.

10-(4,6-Dimethoxy-1,3,5-triazin-2-yl)-10-aza-1,4,7-triazoniacyclododecane Tris(trifluoroacetate) (3). A solution of **2** (1.10 g, 1.80 mmol) in dichloromethane (60 mL) was treated under nitrogen with trifluoroacetic acid (TFA; 5.8 mL, 8.62 g, 75.60 mmol), and the mixture was stirred for 18 h at room temperature. The solvent and the excess of TFA were removed under vacuum. The product **3** was obtained quantitatively as a colorless, hygroscopic solid: yield 1.18 g (quantitative); mp 137 °C; IR (KBr) $\tilde{\nu}$ [cm^{-1}] 2969, 1685, 1201, 1132, 796, 723; UV/vis (CH_3CN) λ_{max} [nm] (log ϵ) 223 (3.452); ^{1}H NMR (300 MHz, CD_3CN) δ 3.14 (bs, 8 H, CH_2−cyclen), 3.19−3.24 (m, 4 H, CH_2−cyclen), 3.88−3.91 (m, 10 H, CH_2−cyclen and OCH_3), 7.55 (bs, 6 H, NH_2^+); ^{1}H NMR (400 MHz, MeOH-d_4) δ 3.19−3.24 (m, 8 H, CH_2−cyclen), 3.30−3.37 (m, 4 H, CH_2−cyclen and solvent MeOH), 3.98 (s, 6 H, OCH_3), 4.10−4.27 (m, 4 H, CH_2−cyclen), 4.99 (bs, 6 H, NH_2^+ and solvent MeOH); ^{1}H NMR (300 MHz, D_2O) δ 3.05−3.12 (m, 4 H, CH_2−cyclen), 3.17−3.21 (m, 8 H, CH_2−cyclen), 3.83−3.94 (m, 10 H, CH_2−cyclen and OCH_3); ^{13}C NMR (75 MHz, CD_3CN) δ 44.6, 45.5, 47.0, 48.7 (−, CH_2−cyclen), 56.1 (+, OCH_3), 116.9 (C_{quat}, q, $^1J_{C,F}$ = 287.2 Hz, CF_3COO^-), 160.6 (C_{quat}, q, $^2J_{C,F}$ = 37.9 Hz, CF_3COO^-), 169.3 (C_{quat}, C_{aryl}−N), 171.3 (C_{quat}, C_{aryl}−OCH_3); ^{13}C NMR (100 MHz, MeOH-d_4) δ 44.6, 46.1, 47.1, 48.4 (−, CH_2−cyclen), 55.7 (+, OCH_3), 117.4 (C_{quat}, q, $^1J_{C,F}$ = 289.6 Hz, CF_3COO^-), 161.6 (C_{quat}, q, $^2J_{C,F}$ = 36.8 Hz, CF_3COO^-), 170.4 (C_{quat}, C_{aryl}−N), 172.4 (C_{quat}, C_{aryl}−OCH_3); ^{13}C NMR (75 MHz, D_2O) δ 43.6, 44.3, 45.4, 47.9 (−, CH_2−cyclen), 56.7 (+, OCH_3), 116.1 (C_{quat}, q, $^1J_{C,F}$ = 288.3 Hz, CF_3COO^-), 162.6 (C_{quat}, q, $^2J_{C,F}$ = 37.4 Hz, CF_3COO^-), 164.6 (C_{quat}, C_{aryl}−N), 167.0 (C_{quat}, C_{aryl}−OCH_3); MS (ESI, CH_3CN) *m*/*z* (%) 312 (100) [M^{3+} − 2H]$^+$, 334 (10) [M^{3+} − 3H + Na]$^+$.

1-(4,6-Dimethoxy-1,3,5-triazin-2-yl)-1,4,7,10-tetraazacyclododecane (L1). A basic ion-exchange resin (OH^- capacity 0.9 mmol/mL) was swollen in water for 15 min and then washed several times. A chromatography column was charged with resin (15 mL). A solution of **3** (0.92 g, 1.37 mmol) in water (30 mL) was slowly passed through this column, followed by a solution of water and acetonitrile. The organic solvent was removed under reduced pressure and the aqueous solvent by lyophilization to give a colorless solid: yield 0.42 g (98%); mp 103 °C; IR (KBr) $\tilde{\nu}$ [cm^{-1}] 3441, 2924, 2856, 1556, 1486, 1359, 806; UV/vis (CH_3CN) λ_{max} [nm] (log ϵ) 234 (2.732); ^{1}H NMR (300 MHz, MeOH-d_4) δ 2.64−

(19) Subat, M.; Borowik, A. S.; König, B. *J. Am. Chem. Soc.* **2004**, *126*, 3185.
(20) Turygin, D. S.; Subat, M.; Raitman, O. A.; Arslanov, V. V.; König, B.; Kalinina, M. A. *Angew. Chem.* **2006**, *118*, 5466.
(21) Subat, M.; König, B. *Synthesis* **2001**, *12*, 1818.

2.74 (m, 8 H, CH_2−cyclen), 2.95−2.99 (m, 4 H, CH_2−cyclen), 3.82−3.89 (m, 4 H, CH_2−cyclen), 3.94 (s, 6 H, OCH_3); ^{1}H NMR (400 MHz, $CDCl_3$) δ 2.66−2.68 (m, 4 H, CH_2−cyclen), 2.77−2.80 (m, 4 H, CH_2−cyclen), 2.96−2.99 (m, 4 H, CH_2−cyclen), 3.80−3.83 (m, 4 H, CH_2−cyclen), 3.94 (s, 6 H, OCH_3); ^{13}C NMR (75 MHz, MeOH-d_4) δ 47.1, 48.7, 49.5, 50.5 (−, CH_2−cyclen), 55.2 (+, OCH_3), 169.8 (C_{quat}, C_{aryl}−N), 173.1 (C_{quat}, C_{aryl}−OCH_3); ^{13}C NMR (100 MHz, $CDCl_3$) δ 47.2, 47.8, 48.8, 49.8 (−, CH_2−cyclen), 54.5 (+, OCH_3), 167.2 (C_{quat}, C_{aryl}−N), 171.9 (C_{quat}, C_{aryl}−OCH_3); MS (ESI, MeOH + 1% AcOH) *m*/*z* (%) 312 (100) $[MH]^+$, 334 (7) $[M + Na]^+$. HRMS ($C_{13}H_{26}N_7O_2$): calcd, 312.2148 $[MH]^+$; obsd, 312.2146 $[MH]^+$ ±0.88 ppm.

[ZnL1](ClO$_4$)$_2$·H$_2$O. A solution of **L1** (0.315 g, 1.01 mmol) in methanol (15 mL) was treated under stirring with a solution of $Zn(ClO_4)_2·6H_2O$ (0.376 g, 1.01 mmol) in methanol (10 mL). A colorless precipitate immediately appeared. The mixture was refluxed for 3 h. Colorless crystals were obtained after recrystallization from a mixture of MeOH/water (4:1). Some petroleum ether was added to the filtrate solution to yield also colorless crystals. Both filter residues showed the same analytical purity: yield 0.554 g (95%); mp 284 °C (dec); IR (KBr) $\tilde{\nu}$ [cm^{-1}] 3428, 3293, 2943, 1576, 1469, 1287, 1140, 812, 627; UV/vis (CH_3CN) λ_{max} [nm] (log ϵ) 226 (3.935); ^{1}H NMR (300 MHz, DMSO-d_6) δ 2.66−2.70 (m, 4 H, CH_2−cyclen), 2.82−2.89 (m, 4 H, CH_2−cyclen), 3.41−3.44 (m, 4 H, CH_2−cyclen and H_2O), 3.89 (s, 6 H, OCH_3), 3.98−4.08 (m, 4 H, CH_2−cyclen); ^{13}C NMR (75 MHz, DMSO-d_6) δ 44.9, 45.5, 46.2, 47.2 (−, CH_2−cyclen), 54.2 (+, OCH_3), 169.0 (C_{quat}, C_{aryl}−N), 171.1 (C_{quat}, C_{aryl}−OCH_3); MS (ESI, CH_2Cl_2/MeOH + 10 mmol/L of NH_4Ac) *m*/*z* (%) 434 (100) $[M^{2+} + CH_3COO^-]^+$, 187 (85) $[M]^{2+}$, 474 (8) $[M^{2+} + ClO_4^-]^+$; MS (ESI, negative, CH_2Cl_2/MeOH + 10 mmol/L of NH_4Ac) *m*/*z* (%) 674 (100) $[M^{2+} + 3ClO_4^-]^-$, 634 (8) $[M^{2+} + 2ClO_4^- + CH_3COO^-]^-$. HRMS ($C_{13}H_{25}N_7O_6Cl_1Zn_1$): calcd, 474.0846 $[M^{2+} + ClO_4^-]^+$; obsd, 474.0842 $[M^{2+} + ClO_4^-]^+$ ±0.95 ppm. Anal. Calcd for $C_{13}H_{25}N_7O_{10}Cl_2Zn·H_2O$: C, 26.30; H, 4.58; N, 16.52. Found: C, 26.38; H, 4.49; N, 16.41.

[CuL1](ClO$_4$)$_2$·H$_2$O. A procedure analogous to that described for **ZnL1** was followed starting from a solution of **L1** (0.15 g, 0.5 mmol) in ethanol (2 mL) and a solution of $Cu(ClO_4)_2·6H_2O$ (0.18 g, 0.5 mmol) in ethanol (3 mL). The resulting blue mixture was refluxed for 18 h. After cooling, the solid compound was filtered off, washed with ethanol, and dried under vacuum to obtain the product as a pale-blue solid: yield 0.28 g (0.49 mmol, 98%); mp 194−196 °C; IR (ATR unit) $\tilde{\nu}$ [cm^{-1}] 3313, 3270, 2941, 1604, 1561, 1486, 1381, 1099, 815, 621; UV/vis (Millipore H_2O) λ_{max} [nm] (log ϵ) 229 (3.889), 272 (3.368), 641 (2.064), 650 (2.033); MS (ESI, H_2O/CH_3CN) *m*/*z* (%) 186.8 (65) $[M]^{2+}$, 207.4 (100) $[M^{2+} + CH_3CN]^{2+}$, 473 (15) $[M^{2+} + ClO_4^-]^+$; MS (ESI, negative, H_2O/CH_3CN) *m*/*z* (%) 672.8 (100) $[M^{2+} + 3ClO_4^-]^-$. Anal. Calcd for $C_{13}H_{25}N_7O_{10}Cl_2Cu·H_2O$: C, 26.44; H, 4.61; N, 16.61. Found: C, 26.53; H, 4.74; N, 16.70.

[NiL1](ClO$_4$)$_2$·2H$_2$O. A procedure analogous to that described for **CuL1** was followed starting from a solution of **L1** (0.127 g, 0.4 mmol) in ethanol (2 mL) and a solution of $Ni(ClO_4)_2·6H_2O$ (0.15 g, 0.4 mmol) in ethanol (3 mL). The resulting turquoise mixture was refluxed for 24 h. After evaporation of the solvent, the product was dried under vacuum to obtain a pale-green, hygroscopic solid: yield 0.158 g (70%); mp 242 °C (dec); IR (KBr) $\tilde{\nu}$ [cm^{-1}] 3398, 3270, 2940, 2360, 1585, 1479, 1366, 1091, 974, 809, 626; UV/vis (Millipore H_2O) λ_{max} [nm] (log ϵ) 228 (4.175), 368 (1.514), 590 (1.212), 964 (1.447); MS (ESI, H_2O/CH_3CN) *m*/*z* (%) 184.3 (60) $[M^{2+}]^{2+}$, 204.9 (100) $[M^{2+} + CH_3CN]^{2+}$, 225.3 (15) $[M^{2+} + 2CH_3CN]^{2+}$, 468 (25) $[M^{2+} + ClO_4^-]^+$; MS (ESI, negative, H_2O/CH_3CN) *m*/*z* (%) 667.9 (100) $[M^{2+} + 3ClO_4^-]^-$. HRMS ($C_{13}H_{25}N_7O_6ClNi$): calcd, 468.0908 $[M^{2+} + ClO_4^-]^+$; obsd, 474.0906 $[M^{2+} + ClO_4^-]^+$ ±0.48 ppm. Anal. Calcd for $C_{13}H_{25}N_7O_{10}Cl_2Ni·2H_2O$: C, 25.81; H, 4.83; N, 16.21. Found: C, 25.31; H, 5.04; N, 16.02.

4,6-Bis(1,4,7,10-tetraazacyclododecane-1,4,7-tricarboxylic acid tri-*tert*-butyl ester)-2-methoxy-1,3,5-triazine (5). A procedure analogous to that described for **2** was followed starting from a solution of **4**[20] (5.28 g, 5.00 mmol) in absolute methanol (50 mL) and NaOMe (0.41 g, 7.59 mmol) under nitrogen. The solvent was removed under vacuum, and the residue was purified by chromatography on silica (ethyl acetate/petroleum ether, 1:4 to 4:1) to give a colorless solid (R_f = 0.47, ethyl acetate/petroleum ether, 1:1); yield 5.17 g (98%); mp 109 °C; IR (KBr) $\tilde{\nu}$ [cm^{-1}] 2976, 2933, 1695, 1571, 1365, 1163, 739; UV/vis (CH_3CN) λ_{max} [nm] (log ϵ) 234 (4.617); ^{1}H NMR (400 MHz, $CDCl_3$) δ 1.37 (s, 18 H, CH_3−Boc), 1.41 (s, 36 H, CH_3−Boc), 3.27−3.62 (m, 32 H, CH_2−cyclen), 3.85 (s, 3 H, OCH_3); ^{13}C NMR (100 MHz, $CDCl_3$) δ 28.4, 28.5 (+, CH_3−Boc), 50.1 (−, vb, CH_2−cyclen), 53.9 (+, OCH_3), 79.9, 80.0 (C_{quat}, C−Boc), 156.3 (C_{quat}, C=O−Boc), 166.3 (C_{quat}, C_{aryl}−N), 170.6 (C_{quat}, C_{aryl}−OCH_3); MS (ESI, MeOH + 1% AcOH) *m*/*z* (%) 1052 (100) $[MH]^+$, 952 (7) $[MH - Boc]^+$. Anal. Calcd for $C_{50}H_{89}N_{11}O_{13}$: C, 57.05; H, 8.52; N, 14.64. Found: C, 57.28; H, 8.37; N, 14.21.

[4,6-Bis(10-aza-1,4,7-triazoniacyclododecan-10-yl)-1,3,5-triazin-2-yl] Methyl Ether Hexakis(trifluoroacetate) (6). A procedure analogous to that described for **3** was followed. The product **6** was obtained quantitatively as a colorless, hygroscopic solid: mp 124 °C; IR (KBr) $\tilde{\nu}$ [cm^{-1}] 2961, 1681, 1208, 1145, 781; UV/vis (CH_3CN) λ_{max} [nm] (log ϵ) 224 (4.502); ^{1}H NMR (250 MHz, D_2O) δ 3.02−3.09 (m, 16 H, CH_2−cyclen), 3.15−3.18 (m, 8 H, CH_2−cyclen), 3.81−3.94 (m, 11 H, CH_2−cyclen and OCH_3); ^{1}H NMR (300 MHz, CD_3CN) δ 3.01−3.17 (m, 16 H, CH_2−cyclen), 3.28−3.39 (m, 16 H, CH_2−cyclen), 3.85 (s, 3 H, OCH_3), 7.17 (bs, 12 H, NH_2^+); ^{13}C NMR (62 MHz, D_2O) δ 43.4, 44.4, 45.6, 47.3 (−, CH_2−cyclen), 55.7 (+, OCH_3), 116.2 (C_{quat}, q, $^1J_{C,F}$ = 291.7 Hz, CF_3COO^-), 162.5 (C_{quat}, q, $^2J_{C,F}$ = 35.6 Hz, CF_3COO^-), 164.5 (C_{quat}, C_{aryl}−N), 166.4 (C_{quat}, C_{aryl}−OCH_3); ^{13}C NMR (75 MHz, CD_3CN) δ 43.6, 43.9, 45.3, 45.9, 46.0, 47.1, 47.4, 47.6 (−, CH_2−cyclen), 55.0 (+, OCH_3), 117.4 (C_{quat}, q, $^1J_{C,F}$ = 291.2 Hz, CF_3COO^-), 161.0 (C_{quat}, q, $^2J_{C,F}$ = 35.8 Hz, CF_3COO^-), 169.8 (C_{quat}, C_{aryl}−N), 171.8 (C_{quat}, C_{aryl}−OCH_3); MS (ESI, CH_3CN) *m*/*z* (%) 452 (100) $[M^{6+} - 5H]^+$, 226 (95) $[M^{6+} - 4H]^{2+}$.

2-Methoxy-4,6-bis(1,4,7,10-tetraazacyclododecan-1-yl)-1,3,5-triazine (L2). A procedure analogous to that described for **L1** was followed. The free amine **L2** was obtained quantitatively as a colorless solid: mp 83 °C; IR (KBr) $\tilde{\nu}$ [cm^{-1}] 3396, 2926, 2841, 1583, 1116, 812, 722; UV/vis (CH_3CN) λ_{max} [nm] (log ϵ) 232 (4.531); ^{1}H NMR (300 MHz, MeOH-d_4) δ 2.65−2.73 (m, 16 H, CH_2−cyclen), 2.87−2.96 (m, 8 H, CH_2−cyclen), 3.75−3.85 (m, 8 H, CH_2−cyclen), 3.89 (s, 3 H, OCH_3); ^{1}H NMR (300 MHz, $CDCl_3$) δ 2.62−2.65 (m, 8 H, CH_2−cyclen), 2.74−2.78 (m, 8 H, CH_2−cyclen), 2.90−2.94 (m, 8 H, CH_2−cyclen), 3.72−3.76 (m, 8 H, CH_2−cyclen), 3.84 (s, 3 H, OCH_3); ^{13}C NMR (75 MHz, D_2O) δ 45.5, 47.5, 48.3, 49.6 (−, CH_2−cyclen), 52.9 (+, OCH_3), 167.1 (C_{quat}, C_{aryl}−N), 170.3 (C_{quat}, C_{aryl}−OCH_3); MS (ESI, MeOH + 10 mmol/L of NH_4Ac) *m*/*z* (%) 452 (100) $[MH]^+$, 226 (8) $[M + 2H]^{2+}$. HRMS ($C_{20}H_{42}N_{11}O_1$): calcd, 452.3574 $[MH]^+$; obsd, 452.3578 $[MH]^+$ ±0.56 ppm.

[Zn$_2$L2](ClO$_4$)$_4$·CH$_3$CN. A procedure analogous to that described for **ZnL1** was followed. A solution of **L2** (0.61 g, 1.35 mmol) in methanol (15 mL) was treated under intense stirring with a solution of $Zn(ClO_4)_2·6H_2O$ (1.06 g, 2.70 mmol) in methanol

(15 mL). Colorless crystals were obtained after recrystallization from a mixture of MeOH/water/acetonitrile (8:1:1). The filtrate solution was reduced to half its volume, and some petroleum ether was added to yield additional product as colorless crystals. Both filter residues showed the same analytical purity: yield 1.29 g (98%); mp 248 °C; IR (KBr) $\tilde{\nu}$ [cm^{-1}] 3600, 3435, 3292, 2931, 1572, 1471, 1350, 1076, 814, 628; UV/vis (CH_3CN) λ_{max} [nm] (log ϵ) 226 (4.735); ^1H NMR (600 MHz, CH_3CN) δ 2.70−2.74 (m, 4 H, CH_2−cyclen), 2.85−2.89 (m, 8 H, CH_2−cyclen), 3.04−3.06 (m, 8 H, CH_2−cyclen), 3.18−3.22 (m, 4 H, CH_2−cyclen), 3.36−3.38 (m, 4 H, CH_2−cyclen), 3.51−3.53 (t, 2 H, ^3J = 5.4 Hz, NH), 3.59 (bs, 4 H, NH), 3.98 (s, 3 H, OCH_3), 4.48−4.51 (m, 4 H, CH_2−cyclen); ^{13}C NMR (150 MHz, CD_3CN) δ 44.4 (−, CH_2−cyclen), 47.0 (−, CH_2−cyclen), 47.8 (−, CH_2−cyclen), 55.8 (+, OCH_3), 172.0 (C_{quat}, C_{aryl}−N), 172.4 (C_{quat}, C_{aryl}−OCH_3); MS (ESI, CH_3CN) *m*/*z* (%) 349 (100) $[M^{4+} + 2CH_3COO^-]^{2+}$, 319 (60) $[M^{4+} - H + CH_3COO^-]^{2+}$; MS (ESI, negative, CH_3CN) *m*/*z* (%) 1038 (100) $[M^{4+} + 4ClO_4^- + CH_3COO^-]^-$, 1078 (15) $[M^{4+} + 5ClO_4^-]^-$. Anal. Calcd for $C_{20}H_{41}N_{11}O_{17}Cl_4Zn_2 \cdot CH_3CN$: C, 25.98; H, 4.36; N, 16.54. Found: C, 26.25; H, 4.66; N, 16.74.

$[Cu_2L2](ClO_4)_4 \cdot 2H_2O$. A procedure analogous to that described for **CuL1** was followed. A solution of **L2** (0.115 g, 0.25 mmol) in ethanol (4 mL) was treated under intense stirring with a solution of $Cu(ClO_4)_2 \cdot 6H_2O$ (0.19 g, 0.5 mmol) in ethanol (3 mL). The resulting dark-blue solution was stirred at room temperature for 2 h and then refluxed for 1 h. The solid compound was filtered off, washed with ethanol, and dried under vacuum to obtain a blue solid: yield 0.185 g (77%); mp 235 °C; IR (ATR unit) $\tilde{\nu}$ [cm^{-1}] 3267, 2959, 2884, 1556, 1469, 1332, 1070, 826, 621; UV/vis (Millipore H_2O) λ_{max} [nm] (log ϵ) 230 (4.355), 650 (2.490); MS (ESI, H_2O/CH_3CN) *m*/*z* (%) 216 (75) $[M^{4+} + 7CH_3CN]^{4+}$, 253 (55) $[M^{4+} + ClO_4^- + 2CH_3CN]^{3+}$, 266 (100) $[M^{4+} + ClO_4^- + 3CH_3CN]^{3+}$, 356 (50) $[M^{4+} + ClO_4^- + Cl^-]^{2+}$, 388 (100) $[M^{4+} + 2ClO_4^-]^{2+}$; MS (ESI, negative, H_2O/CH_3CN) *m*/*z* (%) 1076 (100) $[M^{4+} + 5ClO_4^-]^-$. Anal. Calcd for $C_{20}H_{41}N_{11}O_{17}Cl_4Cu_2 \cdot 2H_2O$: C, 23.79; H, 4.49; N, 15.27. Found: C, 24.01; H, 4.69; N, 15.22.

$[Ni_2L2](ClO_4)_4$. A procedure analogous to that described for **NiL1** was followed. A solution of **L2** (0.105 g, 0.23 mmol) in ethanol (6 mL) was treated under intense stirring with a solution of $Ni(ClO_4)_2 \cdot 6H_2O$ (0.17 g, 0.46 mmol) in ethanol (6 mL). The resulting pale-blue solution was refluxed for 24 h. After reflux, the solution and the residue were green. The solid compound was filtered off, washed with ethanol, and dried under vacuum to obtain the product as a green, hygroscopic solid: yield 0.155 g (72%); mp 222 °C; IR (KBr) $\tilde{\nu}$ [cm^{-1}] 3421, 3279, 2949, 2889, 2023, 1568, 1458, 1408, 1349, 1105, 1091, 980, 927, 816, 626; UV/vis (Millipore H_2O) λ_{max} [nm] (log ϵ) 228 (4.205), 361 (1.970), 589 (1.970); MS (ESI, H_2O/CH_3CN) *m*/*z* (%) 203.2 (85) $[M^{4+} + 6CH_3CN]^{4+}$, 241.7 (100) $[M^{4+} + Cl^- + 3CH_3CN]^{3+}$, 263.1 (80) $[M^{4+} + ClO_4^- + 3CH_3CN]^{3+}$, 351.4 (70) $[M^{4+} + ClO_4^- + Cl^-]^{2+}$, 383.5 (30) $[M^{4+} + 2ClO_4^-]^{2+}$, 802.2 (15) $[M^{4+} + 2ClO_4^- + Cl^-]^+$; MS (ESI, negative, H_2O/CH_3CN) *m*/*z* (%) 937.9 (55) $[M^{4+} + 3ClO_4^- + 2Cl^-]^-$, 1002 (100) $[M^{4+} + 4ClO_4^- + Cl^-]^-$, 1064 (60) $[M^{4+} + 5ClO_4^-]^-$. HRMS ($C_{20}H_{39}N_{11}ClO_5Ni_2$): calcd, 664.1531 $[M^{4+} + ClO_4^- - 2H^+]^+$; obsd, 664.1518 $[M^{4+} + ClO_4^- - 2H^+]^+ \pm 1.96$ ppm.

10-[4-Chloro-6-(1,4,7,10,13-pentaoxa-16-azacyclooctadecan-16-yl)-1,3,5-triazin-2-yl]-1,4,7,10-tetraazacyclododecane-1,4,7-tricarboxylic Acid Tri-*tert*-butyl Ester (7). A solution of **1** (2.0 g, 3.22 mmol) and 1-aza-18-crown-6 (0.85 g, 3.22 mmol) in acetone (15 mL) was treated under nitrogen with K_2CO_3 (0.67 g, 4.83 mmol), and the mixture was refluxed for 3 h. The solvent was removed under vacuum, and the residue was purified by chromatography on silica (ethyl acetate/methanol, 98:2) to give a colorless solid (R_f = 0.16; ethyl acetate/methanol, 95:5): yield 2.45 g (91%); mp 153 °C; IR (KBr) $\tilde{\nu}$ [cm^{-1}] 3446, 2974, 2870, 1695, 1570, 1249, 1133, 972, 803, 778; UV/vis (CH_3CN) λ_{max} [nm] (log ϵ) 234 (4.574); ^1H NMR (300 MHz, $CDCl_3$) δ 1.43 (s, 18 H, CH_3−Boc), 1.47 (s, 9 H, CH_3−Boc), 3.39−3.51 (m, 12 H, CH_2−cyclen), 3.62−3.75 (m, 24 H, CH_2−azacrown), 3.83−3.87 (m, 4 H, CH_2−cyclen); ^{13}C NMR (75 MHz, $CDCl_3$) δ 28.4, 28.5 (+, CH_3−Boc), 48.0, 48.3, 50.0, 50.5, 50.9, 51.0 (−, CH_2−cyclen and CH_2−azacrown), 69.1, 69.4, 70.4, 70.5, 70.5, 70.6, 70.7, 70.8 (−, CH_2−azacrown), 80.0, 80.3 (C_{quat}, C−Boc), 156.3, 157.2 (C_{quat}, C═O−Boc), 164.6, 165.0 (C_{quat}, C_{aryl}−N), 168.9 (C_{quat}, C_{aryl}−Cl); MS (FAB, CH_2Cl_2/MeOH, glycerin) *m*/*z* (%) 847 (100) $[MH]^+$, 547 (35) $[MH - 3Boc]^+$, 747 (11) $[MH - Boc]^+$, 869 (5) $[M + Na]^+$. Anal. Calcd for $C_{38}H_{67}N_8O_{11}Cl_1$: C, 53.87; H, 7.97; N, 13.22. Found: C, 54.21; H, 8.17; N, 13.67.

10-[4-Methoxy-6-(1,4,7,10,13-pentaoxa-16-azacyclooctadecan-16-yl)-1,3,5-triazin-2-yl]-1,4,7,10-tetraazacyclododecane-1,4,7-tricarboxylic Acid Tri-*tert*-butyl Ester (8). A procedure analogous to that described for **2** was followed starting from a solution of **7** (2.05 g, 2.42 mmol) in absolute methanol (20 mL) and NaOMe (0.21 g, 3.89 mmol) under nitrogen. The residue was suspended in a solution of ethyl acetate/methanol (98:2) and filtered through a very small amount of silica in order to avoid adsorption of the polar product on the silica. Product **8** was isolated as a colorless solid (R_f = 0.25, ethyl acetate/methanol, 95:5): yield 2.02 g (99%); mp 81 °C; IR (KBr) $\tilde{\nu}$ [cm^{-1}] 3495, 2975, 2869, 1692, 1573, 1250, 1167, 974, 814, 778; UV/vis (CH_3CN) λ_{max} [nm] (log ϵ) 231 (4.538); ^1H NMR (300 MHz, $CDCl_3$) δ 1.41 (s, 18 H, CH_3−Boc), 1.47 (s, 9 H, CH_3−Boc), 3.22−3.52 (m, 12 H, CH_2−cyclen), 3.61−3.69 (m, 24 H, CH_2−azacrown), 3.82−3.97 (m, 7 H, OCH_3 and CH_2−cyclen); ^{13}C NMR (75 MHz, $CDCl_3$) δ 28.5, 28.6 (+, CH_3−Boc), 48.1, 48.4, 50.4, 51.9 (−, CH_2−cyclen and CH_2−azacrown), 53.9 (+, OCH_3), 69.6, 69.7, 70.5, 70.6, 70.7, 70.9 (−, CH_2−azacrown), 79.8, 80.1 (C_{quat}, C−Boc), 156.3, 156.9 (C_{quat}, C═O−Boc), 165.7, 166.6 (C_{quat}, C_{aryl}−N), 170.4 (C_{quat}, C_{aryl}−OCH_3); MS (ESI, MeOH/CH_2Cl_2 + 1% AcOH) *m*/*z* (%) 844 (100) $[MH]^+$, 866 (5) $[M + Na]^+$. Anal. Calcd for $C_{39}H_{70}N_8O_{12}$: C, 55.56; H, 8.37; N, 13.29. Found: C, 55.22; H, 8.22; N, 13.76.

10-[4-Methoxy-6-(1,4,7,10,13-pentaoxa-16-azacyclooctadecan-16-yl)-1,3,5-triazin-2-yl]-10-aza-1,4,7-triazoniacyclododecane Tris-(trifluoroacetate) (9). A procedure analogous to that described for **3** was followed starting from a solution of **8** (1.52 g, 1.80 mmol) in dichloromethane (30 mL) and TFA (4.2 mL, 6.22 g, 54.53 mmol). The product **9** was obtained quantitatively as pale-yellow, viscous oil: yield 1.62 g (quantitative); UV/vis (CH_3CN) λ_{max} [nm] (log ϵ) 227 (4.472); ^1H NMR (600 MHz, CD_3CN) δ 3.15−3.29 (m, 12 H, CH_2−cyclen and CH_2−azacrown), 3.47−3.99 (m, 28 H, CH_2−cyclen and CH_2−azacrown), 4.07 (s, 3 H, OCH_3), 8.13 (bs, 6 H, NH_2^+); ^1H NMR (300 MHz, MeOH-d_4) δ 3.17−3.22 (m, 8 H, CH_2*), 3.29−3.39 (m, 4 H, CH_2* and solvent MeOH), 3.53−3.64 (m, 16 H, CH_2*), 3.71−3.78 (m, 4 H, CH_2*), 3.86−3.90 (m, 4 H, CH_2*), 3.98−4.01 (m, 7 H, CH_2* and OCH_3); ^1H NMR (250 MHz, D_2O) δ 3.09−3.27 (m, 14 H, CH_2−cyclen and CH_2−azacrown), 3.42−3.77 (m, 22 H, CH_2−cyclen and CH_2−azacrown, 3.81−3.89 (m, 7 H, CH_2−cyclen−CH_2 and OCH_3); ^{13}C NMR (150 MHz, CD_3CN) δ 45.5, 45.7, 47.3, 49.7, 50.4, 52.4 (−, CH_2−cyclen and CH_2−azacrown), 57.5 (+, OCH_3), 68.6, 69.7, 69.9, 70.2, 70.4, 71.0, 71.1, 71.4 (−, CH_2−azacrown), 117.0 (C_{quat}, q, $^1J_{C,F}$ = 289.4 Hz, CF_3COO^-), 157.7 (C_{quat}, C_{aryl}−N), 160.7 (C_{quat}, q, $^2J_{C,F}$ = 37.6 Hz, CF_3COO^-), 163.3 (C_{quat}, C_{aryl}−N), 165.1 (C_{quat}, C_{aryl}−OCH_3); ^{13}C NMR (100 MHz, D_2O) δ 44.0, 44.6, 46.0, 48.0, 49.2 (−, CH_2−cyclen and CH_2−azacrown), 56.7 (+, OCH_3), 67.5, 68.4, 69.4, 69.6,

69.8, 70.1 (−, CH_2−azacrown), 116.4 (C_{quat}, q, $^1J_{C,F}$ = 291.8 Hz, CF_3COO^-), 156.9, 162.2 (C_{quat}, C_{aryl}−N), 162.8 (C_{quat}, q, $^2J_{C,F}$ = 35.4 Hz, CF_3COO^-), 163.8 (C_{quat}, C_{aryl}−OCH_3); MS (ESI, MeOH + 1% AcOH) *m*/*z* (%) 543 (100) $[M^{3+} - 2H]^+$, 272 (33) $[M^{3+} - H]^{2+}$, 565 (21) $[M^{3+} - 3H + Na]^+$. [*A more accurate distinction between the cyclen− and azacrown−CH_2 groups was not possible in this solvent because of a strong overlap of the signals. 2D spectra did not provide further information.]

16-[4-Methoxy-6-(1,4,7,10-tetraazacyclododecan-1-yl)-1,3,5-triazin-2-yl]-1,4,7,10,13-pentaoxa-16-azacyclooctadecane (L3). A procedure analogous to that described for **L1** was followed. A solution of **9** (1.40 g, 1.55 mmol) in water (15 mL) was slowly passed through a column of basic ion-exchange resin. The column was then washed with water (120 mL) and acetonitrile (30 mL). The free amine **L3** was obtained quantitatively as a colorless solid: yield 0.84 g (quantitative); mp 76 °C; IR (KBr) $\tilde{\nu}$ [cm^{-1}] 3440, 2868, 1574, 1358, 1115, 941, 812; UV/vis (CH_3CN) λ_{max} [nm] (log ϵ) 231 (4.501); ^{1}H NMR (600 MHz, MeOH-d_4) δ 2.67−2.68 (m, 4 H, CH_2−cyclen), 2.74−2.76 (m, 4 H, CH_2−cyclen), 2.95−2.97 (m, 4 H, CH_2−cyclen), 3.56−3.65 (m, 8 H, CH_2−azacrown), 3.66−3.69 (m, 8 H, CH_2−cyclen), 3.71−3.75 (m, 4 H, CH_2−azacrown), 3.76−3.79 (m, 4 H, CH_2−cyclen), 3.85−3.89 (m, 4 H, CH_2−azacrown), 3.90 (s, 3 H, OCH_3); ^{13}C NMR (150 MHz, MeOH-d_4) δ 45.8 (−, CH_2−cyclen), 47.6, 47.9 (−, CH_2−cyclen and CH_2−azacrown), 48.2. 48.9 (−, CH_2−cyclen), 52.9 (+, OCH_3), 69.1, 70.1, 70.2, 70.3, 70.4 (−, CH_2−azacrown), 165.8 (C_{quat}, C_{aryl}−$N_{azacrown}$), 167.4 (C_{quat}, C_{aryl}−N_{cyclen}), 170.6 (C_{quat}, C_{aryl}−OCH_3); MS (ESI, MeOH + 10 mmol/L of NH_4Ac) *m*/*z* (%) 543(100) $[MH]^+$, 565 (21) $[M + Na]^+$, 272 (17) $[M + 2H]^{2+}$. HRMS ($C_{24}H_{47}N_8O_6$): calcd, 543.3619 $[MH]^+$; obsd, 543.3624 $[MH]^+$ ±1.23 ppm.

[ZnL3](ClO$_4$)$_2$. A procedure analogous to that described for **ZnL1** was followed. To a solution of **L3** (0.65 g, 1.20 mmol) in methanol (15 mL) were added under intense stirring portions of a solution of $Zn(ClO_4)_2 \cdot 6H_2O$ (0.446 g, 1.20 mmol) in methanol (10 mL). The solution remained clear even after the addition of the Zn salt. The mixture was refluxed for 18 h. After removal of the solvent under vacuum, the residue was washed three times with 2 mL of cold methanol over a sintered-glass funnel. The product was isolated as colorless crystals: yield 0.887 g (92%); mp 181 °C; IR (KBr) $\tilde{\nu}$ [cm^{-1}] 3435, 3269, 2926, 1580, 1471, 1352, 1108, 980, 815, 625; UV/vis (CH_3CN) λ_{max} [nm] (log ϵ) 228 (4.409); ^{1}H NMR (300 MHz, CD_3CN) δ 2.68−3.12 (m, 12 H, CH_2), 3.34−3.86 (m, 26 H, CH_2), 3.92 (s, 3 H, OCH_3), 4.16−4.28 (m, 2 H, CH_2); ^{13}C NMR (75 MHz, CD_3CN) δ 44.8, 46.8, 47.5, 48.9, 49.4 (−, CH_2−cyclen and CH_2−azacrown), 55.4 (+, OCH_3), 70.0, 70.6, 70.7, 70.8, 71.1 (−, CH_2−azacrown), 166.9, 171.8 (C_{quat}, C_{aryl}−N), 172.8 (C_{quat}, C_{aryl}−OCH_3); MS (ESI, CH_3CN) *m*/*z* (%) 665 (100) $[M^{2+} + CH_3COO^-]^+$, 344 (28) $[M^{2+} + CH_3CN]^{2+}$, 705 (10) $[M^{2+} + ClO_4^-]^+$; MS (ESI, negative, CH_3CN) *m*/*z* (%) 865 (100) $[M^{2+} + 2ClO_4^- + CH_3COO^-]^-$; 905 (65) $[M^{2+} + 3ClO_4^-]^-$. HRMS ($C_{24}H_{45}N_8O_6Zn$): calcd, 605.2754 $[M^{2+} - H]^+$; obsd, 605.2756 $[M^{2+} - H]^+$ ±1.48 ppm.

4,6-Bis(1,4,7,10-tetraazacyclododecane-1,4,7-tricarboxylic acid tri-*tert*-butyl ester)-2-(1,4,7,10,13-pentaoxa-16-azacyclooctadecan-16-yl)-1,3,5-triazine (10). A procedure analogous to that described for **7** was followed starting from a solution of **4**[20] (1.2 g, 1.14 mmol), 1-aza-18-crown-6 (0.45 g, 1.71 mmol), and K_2CO_3 (0.47 g, 3.42 mmol) in acetone (25 mL), and the mixture was refluxed for 24 h. The solvent was removed under vacuum, and the residue was purified by chromatography on silica (ethyl acetate/methanol, 97:3) to give a colorless solid (R_f = 0.31; ethyl acetate/methanol, 97:3): yield 1.27 g (87%); mp 97 °C; IR (KBr) $\tilde{\nu}$ [cm^{-1}] 3449, 2975, 2932, 1697, 1541, 1249, 1166, 777; UV/vis (CH_3CN) λ_{max} [nm] (log ϵ) 232 (4.695); ^{1}H NMR (300 MHz, $CDCl_3$) δ 1.38 (s, 18 H, CH_3−Boc), 1.40 (s, 36 H, CH_3−Boc), 3.24−3.88 (m, 56 H, CH_2−cyclen and CH_2−azacrown); ^{13}C NMR (75 MHz, $CDCl_3$) δ 28.5, 28.6 (+, CH_3−Boc), 48.1 (−, CH_2−azacrown), 50.5 (−, CH_2−cyclen), 70.0, 70.5 70.6, 70.7, 70.9 (−, CH_2−azacrown), 79.7, 79.8 (C_{quat}, C−Boc), 156.2 (C_{quat}, C═O−Boc), 164.6, 166.6 (C_{quat}, C_{aryl}−N); MS (ESI, CH_2Cl_2/MeOH + 1% AcOH) *m*/*z* (%) 1284 (100) $[MH]^+$, 1306 (10) $[M + Na]^+$. Anal. Calcd for $C_{61}H_{110}N_{12}O_{17}$: C, 57.08; H, 8.64; N, 13.09. Found: C, 57.25; H, 8.78; N, 13.24.

[4,6-Bis(10-aza-1,4,7-triazoniacyclododecan-10-yl)-1,3,5-triazin-2-yl]-1,4,7,10,13-pentaoxa-16-azacyclooctadecane Hexakis(trifluoroacetate) (11). A procedure analogous to that described for **3** was followed starting from a solution of **10** (0.90 g, 0.70 mmol) in dichloromethane (30 mL) and TFA (3.3 mL, 4.88 g, 42.8 mmol). The product **11** was obtained as a highly viscous oil. The oily residue was dissolved in a small amount of acetonitrile, and the solvent was removed under vacuum. This procedure was repeated three times in order to remove all traces of TFA. Product **11** was obtained quantitatively as a pale-yellow, very hygroscopic solid: yield 0.958 g (quantitative); mp 47−49 °C; IR (KBr) $\tilde{\nu}$ [cm^{-1}] 3429, 2970, 2802, 1571, 1195, 781; UV/vis (CH_3CN) λ_{max} [nm] (log ϵ) 225 (4.221); ^{1}H NMR (300 MHz, CD_3CN) δ 2.98−3.29 (m, 28 H, CH_2−cyclen and CH_2−azacrown), 3.52−3.63 (m, 16 H, CH_2−cyclen and CH_2−azacrown), 3.46−3.79 (m, 8 H, CH_2−cyclen and CH_2−azacrown), 3.95−3.99 (m, 4 H, CH_2−cyclen), 7.74 (bs, 12 H, NH_2^+); ^{13}C NMR (75 MHz, CD_3CN) δ 44.2, 45.0, 46.2, 47.5, 50.5 (−, CH_2−cyclen and CH_2−azacrown), 70.8, 71.1, 71.3, 71.4, 71.5 (−, CH_2−azacrown), 117.0 (C_{quat}, q, $^1J_{C,F}$ = 287.8 Hz, CF_3COO^-), 160.6 (C_{quat}, q, $^2J_{C,F}$ = 36.5 Hz, CF_3COO^-), 162.1, 165.8 (C_{quat}, C_{aryl}−N); MS (ESI, MeOH + 10 mmol/L of NH_4Ac) *m*/*z* (%) 342 (100) $[M^{6+} - 4H]^{2+}$, 683 (30) $[M^{6+} - 5H]^+$, 353 (28) $[M^{6+} - 5H + Na]^{2+}$, 705 (9) $[M^{6+} - 6H + Na]^+$.

16-[4,6-Bis(1,4,7,10-tetraazacyclododecan-1-yl)-1,3,5-triazin-2-yl]-1,4,7,10,13-pentaoxa-16-azacyclooctadecane (L4). A procedure analogous to that described for **L1** was followed. The free amine **L4** was obtained quantitatively as a colorless solid: mp 58 °C; IR (KBr) $\tilde{\nu}$ [cm^{-1}] 3441, 2952, 2867, 1572, 1348, 1125, 773; UV/vis (CH_3CN) λ_{max} [nm] (log ϵ) 228 (4.482); ^{1}H NMR (300 MHz, MeOH-d_4) δ 2.65−2.67 (m, 8 H, CH_2−cyclen), 2.72−2.74 (m, 8 H, CH_2−cyclen), 2.91−2.94 (m, 8 H, CH_2−cyclen), 3.54−3.87 (m, 32 H, CH_2−cyclen and CH_2−azacrown); ^{13}C NMR (75 MHz, MeOH-d_4) δ 47.3, 49.0, 49.5, 49.6, 50.1 (−, CH_2−cyclen and CH_2−azacrown), 70.9, 71.6, 71.7, 71.8, 71.9 (−, CH_2−azacrown), 166.0 (C_{quat}, C_{aryl}−$N_{azacrown}$), 168.0 (C_{quat}, C_{aryl}−N_{cyclen}); MS (ESI, MeOH + 10 mmol/L of NH_4Ac) *m*/*z* (%) 684 (100) $[MH]^+$, 342 (25) $[M + 2H]^{2+}$. HRMS ($C_{31}H_{63}N_{12}O_5$): calcd, 683.6044 $[MH]^+$; obsd, 683.6051 $[MH]^+$ ±0.73 ppm.

[Zn$_2$L4](ClO$_4$)$_4$. A procedure analogous to that described for **Zn$_2$L2** was followed. To a solution of **L4** (0.39 g, 0.57 mmol) in methanol (20 mL) under intense stirring were added portions of a solution of $Zn(ClO_4)_2 \cdot 6H_2O$ (0.424 g, 1.14 mmol) in methanol (12 mL). At the beginning, a colorless precipitate appeared, which dissolved after the addition of the total amount of Zn salt. The mixture was refluxed for 24 h. After removal of all solvents under vacuum, the residue was dissolved in methanol and cooled in an ice bath and some petroleum ether was added to yield the product as colorless crystals: yield 0.571 g (82%); mp 168 °C; IR (KBr) $\tilde{\nu}$ [cm^{-1}] 3537, 3261, 2963, 2883, 1567, 1347, 1085, 814, 627; UV/vis (CH_3CN) λ_{max} [nm] (log ϵ) 225 (4.575); ^{1}H NMR (300 MHz, CD_3CN) δ 2.65−3.16 (m, 24 H, cyclen−CH_2), 3.34−3.91 (m, 34 H, CH_2−cyclen, CH_2−azacrown and NH), 4.24−4.28 (m, 4 H,

CH_2−cyclen); ^{13}C NMR (75 MHz, CD_3CN) δ 44.5, 45.9, 46.8, 48.0, 49.4 (−, CH_2−cyclen and CH_2−azacrown), 70.2, 70.6, 70.7, 71.0, 71.1 (−, CH_2−azacrown), 165.9 (C_{quat}, C_{aryl}−$N_{azacrown}$), 170.9 (C_{quat}, C_{aryl}−N_{cyclen}); MS (ESI, CH_3CN) *m/z* (%) 465 (100) $[M^{4+} + 2CH_3COO^-]^{2+}$, 486 (55) $[M^{4+} + ClO_4^- + CH_3COO^-]^{2+}$, 1071 (10) $[M^{4+} + 2ClO_4^- + CH_3COO^-]^+$; MS (ESI, negative, CH_3CN) 1227 (100) $[M^{4+} + 4ClO_4^- + OH^-]^-$, 1269 (85) $[M^{4+} + 4ClO_4^- + CH_3COO^-]^-$ 1309 (22) $[M^{4+} + 5ClO_4^-]^-$.

2,6-Bis(10-aza-1,4,7-azoniacyclododecan-10-yl)pyridine Hexakis(trifluoroacetate) (13). A procedure analogous to that described for **3** was followed starting from a solution of **12**[21] (0.60 g, 0.59 mmol) in dichloromethane (20 mL) and TFA (2.7 mL, 4.03 g, 35.42 mmol). Compound **13** was isolated quantitatively as a colorless solid: mp 98−100 °C; IR (KBr) $\tilde{\nu}$ [cm^{-1}] 3299, 2995, 2875, 1571, 1196, 778; UV/vis (CH_3CN) λ_{max} [nm] (log ϵ) 221 (4.145), 255 (3.978), 317 (3.981); ^1H NMR (300 MHz, CD_3CN) δ 3.07−3.25 (m, 24 H, CH_2−cyclen), 3.73−3.88 (m, 8 H, CH_2−cyclen), 6.07 (d, 2 H, ^3J = 8.2 Hz, CH−pyridine), 7.34 (t, 1 H, ^3J = 8.2 Hz, CH−pyridine), 8.53 (bs, 12 H, NH_2^+); ^{13}C NMR (75 MHz, CD_3CN) δ 44.5, 45.9, 46.9, 47.8 (−, CH_2−cyclen), 98.7 (+, C_{aryl}−H−pyridine), 117.1 (C_{quat}, q, $^1J_{C,F}$ = 288.1 Hz, CF_3COO^-), 140.7 (+, C_{aryl}−H−pyridine), 158.6 (C_{quat}, C_{aryl}−N−pyridine), 160.7 (C_{quat}, q, $^2J_{C,F}$ = 36.8 Hz, CF_3COO^-); MS (ESI, CH_3CN) *m/z* (%) 420 (100) $[M^{6+} - 5H]^+$, 211 (45) $[M^{6+} - 4H]^{2+}$.

2,6-Bis(1,4,7,10-tetraazacyclododecan-1-yl)pyridine (L5). A procedure analogous to that described for **L1** was followed. A solution of **13** (0.55 g, 0.49 mmol) in water (10 mL) was slowly passed through a column of basic ion-exchange resin (30 mL). The free amine **L5** was obtained as a colorless solid: yield 0.203 g (99%); mp 85 °C; IR (KBr) $\tilde{\nu}$ [cm^{-1}] 3352, 2981, 2874, 1582, 1342, 1212, 777; UV/vis (CH_3CN) λ_{max} [nm] (log ϵ) 225 (4.221), 258 (4.060), 321 (4.167); ^1H NMR (300 MHz, $CDCl_3$) δ 2.62−2.66 (m, 8 H, CH_2−cyclen), 2.76−2.87 (m, 8 H, CH_2−cyclen), 2.91−2.99 (m, 8 H, CH_2−cyclen), 3.62−3.68 (m, 8 H, CH_2−cyclen), 6.07 (d, 2 H, ^3J = 8.1 Hz, CH−pyridine), 7.28 (t, 1 H, ^3J = 8.1 Hz, CH−pyridine and $CDCl_3$); ^{13}C NMR (75 MHz, $CDCl_3$) δ 46.4, 48.1, 48.8, 50.8 (−, CH_2−cyclen), 96.3 (+, C_{aryl}−H−pyridine), 138.4 (+, C_{aryl}−H−pyridine), 158.7 (C_{quat}, C_{aryl}−N−pyridine); MS (ESI, MeOH/CH_2Cl_2 + 1% AcOH) *m/z* (%) 420 (100) $[MH]^+$, 442 (15) $[M + Na]^+$. HRMS ($C_{21}H_{42}N_9$): calcd, 420.3563 $[MH]^+$; obsd, 420.3561 $[MH]^+$ ±0.82 ppm.

$[Zn_2L5](ClO_4)_4 \cdot H_2O$. A procedure analogous to that described for **Zn_2L2** was followed. To a solution of **L5** (0.18 g, 0.43 mmol) in methanol (20 mL) were added slowly under stirring portions of a solution of $Zn(ClO_4)_2 \cdot 6H_2O$ (0.32 g, 0.86 mmol) in methanol (10 mL). A colorless precipitate immediately appeared. The mixture was stirred for 18 h at room temperature and then refluxed for 30 min. The precipitate was dissolved during reflux, and the clear solution became slightly brown. Half of the amount of solvent was removed under vacuum. The mixture was cooled overnight. Colorless crystals were obtained after filtration and were washed with cold methanol: yield 0.216 g (53%); mp 201 °C (dec); IR (KBr) $\tilde{\nu}$ [cm^{-1}] 3580, 3372, 2997, 2878, 1575, 1346, 1211, 779; UV/vis (CH_3CN) λ_{max} [nm] (log ϵ) 223 (4.170), 256 (4.001), 319 (4.121); ^1H NMR (300 MHz, CD_3CN) δ 2.81−2.89 (m, 4 H, CH_2−cyclen), 2.95−3.18 (m, 8 H, CH_2−cyclen), 3.29−3.50 (m, 8 H, CH_2−cyclen), 3.75−3.99 (18 H, CH_2−cyclen and NH), 7.35 (d, 2 H, ^3J = 8.0 Hz, CH−pyridine), 8.06 (t, 1 H, ^3J = 8.1 Hz, CH−pyridine); ^{13}C NMR (75 MHz, CD_3CN) δ 43.9, 44.5, 45.1, 52.9 (−, CH_2−cyclen), 106.9 (+, C_{aryl}−H−pyridine), 141.1 (+, C_{aryl}−H−pyridine), 159.9 (C_{quat}, C_{aryl}−N−pyridine); MS (ESI, CH_3CN) *m/z* (%) 215 (100) $[M^{4+} + ClO_4^-]^{3+}$, 229 (80) $[M^{4+} + ClO_4^- + CH_3CN]^{3+}$. Anal. Calcd for $C_{21}H_{41}N_9O_{16}Cl_4Zn_2 \cdot H_2O$: C, 26.11; H, 4.49; N, 13.05. Found: C, 25.98; H, 4.45; N, 12.81.

6,6′-Bis(10-aza-1,4,7-triazoniacyclododecan-10-yl)-2,2′-bipyridine Hexakis(trifluoroacetate) (15). A procedure analogous to that described for **3** was followed starting from a solution of **14**[21] (1.20 g, 1.09 mmol) in dichloromethane (40 mL) and TFA (5 mL, 7.48 g, 65.63 mmol). After the addition of TFA, the solution is colored intensively yellow. The solvent and the excess of TFA were removed under vacuum. The salt **15** was isolated quantitatively as a yellow, viscous oil: yield 1.29 g (quantitative); IR (KBr) $\tilde{\nu}$ [cm^{-1}] 3432, 3261, 2915, 2878, 1677, 1615, 1435, 1201, 787, 718; UV/vis (CH_3CN) λ_{max} [nm] (log ϵ) 227 (4.170), 259 (3.237), 339 (3.091); ^1H NMR (400 MHz, CD_3CN) δ 3.16−3.18 (m, 8 H, CH_2−cyclen), 3.25−3.28 (m, 16 H, CH_2−cyclen), 3.89−3.94 (m, 8 H, CH_2−cyclen), 7.02 (d, 2 H, ^3J = 8.7 Hz, CH−pyridine), 7.56 (d, 2 H, ^3J = 7.3 Hz, CH−pyridine), 7.88 (dd, 2 H, ^3J = 8.7 and 7.3 Hz, CH−pyridine), 8.54 (bs, 12 H, NH_2^+); ^1H NMR (250 MHz, D_2O) δ 3.06−3.10 (m, 8 H, CH_2−cyclen), 3.15−3.19 (m, 16 H, CH_2−cyclen), 3.78−3.82 (m, 8 H, CH_2−cyclen), 7.04 (d, 2 H, ^3J = 8.9 Hz, CH−pyridine), 7.53 (d, 2 H, ^3J = 7.5 Hz, CH−pyridine), 7.87 (dd, 2 H, ^3J = 8.9 and ^3J = 7.5 Hz, CH−pyridine); ^{13}C NMR (100 MHz, CD_3CN) δ 45.5, 45.6, 47.1, 50.4 (−, CH_2−cyclen), 112.0 (+, C_{aryl}−H−pyridine), 112.7 0 (+, C_{aryl}−H−pyridine), 118.4 (C_{quat}, q, $^1J_{C,F}$ = 289.9 Hz, CF_3COO^-), 142.4 0 (+, C_{aryl}−H−pyridine), 148.1 (C_{quat}, C_{aryl}−N−pyridine), 156.9 (C_{quat}, C_{aryl}−N−pyridine), 161.0 (C_{quat}, q, $^2J_{C,F}$ = 36.9 Hz, CF_3COO^-); ^{13}C NMR (63 MHz, D_2O) δ 43.9, 44.3, 45.4, 48.8 (−, CH_2−cyclen), 112.3, 113.0 (+, C_{aryl}−H−pyridine), 116.2 (C_{quat}, q, $^1J_{C,F}$ = 291.2 Hz, CF_3COO^-), 142.9 (+, C_{aryl}−H−pyridine), 143.5 (C_{quat}, C_{aryl}−N−pyridine), 154.9 (C_{quat}, C_{aryl}−N−pyridine), 162.6 (C_{quat}, q, $^2J_{C,F}$ = 35.9 Hz, CF_3COO^-); MS (ESI, MeOH/H_2O + 10 mmol/L of NH_4Ac) *m/z* (%) 497 (100) $[M^{6+} - 5H]^+$, 249 (50) $[M^{6+} - 4H]^{2+}$.

6,6′-Bis(1,4,7,10-tetraazacyclododecan-1-yl)-2,2′-bipyridine (L6). A procedure analogous to that described for **L1** was followed. A solution of **15** (1.10 g, 0.93 mmol) in water (25 mL) was slowly passed through a column of basic ion-exchange resin (60 mL). The free amine **L6** was obtained as a pale-yellow solid: yield 0.451 g (98%); mp 95 °C; IR (KBr) $\tilde{\nu}$ [cm^{-1}] 3415, 2926, 2833, 1651, 1574, 1471, 1363, 787, 737; UV/vis (CH_3CN) λ_{max} [nm] (log ϵ) 230 (3.877), 269 (3.675), 351 (3.391); ^1H NMR (400 MHz, MeOH-d_4) δ 2.61−2.64 (m, 8 H, CH_2−cyclen), 2.71−2.73 (m, 8 H, CH_2−cyclen), 2.95−3.19 (m, 8 H, CH_2−cyclen), 3.68−3.73 (m, 8 H, CH_2−cyclen), 6.83 (d, 2 H, ^3J = 8.4 Hz, CH−pyridine), 7.62 (dd, 2 H, ^3J = 8.4 and 7.4 Hz, CH−pyridine), 7.73 (d, 2 H, ^3J = 7.4 Hz, CH−pyridine); ^{13}C NMR (100 MHz, MeOH-d_4) δ 46.8, 48.4, 49.0, 51.6 (−, CH_2−cyclen), 109.8 (+, C_{aryl}−H−pyridine), 111.6 (+, C_{aryl}−H−pyridine), 139.2 (+, C_{aryl}−H−pyridine), 155.6 (C_{quat}, C_{aryl}−N−pyridine), 160.7 (C_{quat}, C_{aryl}−N−pyridine); MS (ESI, MeOH + 10 mmol/L of NH_4Ac) *m/z* (%) 497 (100) $[MH]^+$, 249 (60) $[M + 2H]^{2+}$. HRMS ($C_{26}H_{45}N_{10}$): calcd, 497.3829 $[MH]^+$; obsd, 497.3828 $[MH]^+$ ±0.49 ppm.

$[Zn_2L6](ClO_4)_4 \cdot H_2O$. A procedure analogous to that described for **Zn_2L2** was followed. To a solution of **L6** (0.38 g, 0.77 mmol) in methanol (20 mL) were added slowly under intense stirring portions of a solution of $Zn(ClO_4)_2 \cdot 6H_2O$ (0.57 g, 1.53 mmol) in methanol (15 mL). A colorless precipitate immediately appeared. The mixture was stirred for 22 h at room temperature and then refluxed for 4 h. The solvent was removed under vacuum. Pale-yellow crystals were obtained after recrystallization from a mixture of MeOH/water (4:1). The concentrated filtrate solution showed the same analytical purity of the product, and thus both fractions were united: yield 0.765 g (98%); mp 235−237 °C; IR (KBr) $\tilde{\nu}$ [cm^{-1}] 3429, 2945, 2869, 1649, 1576, 1468, 1362, 786, 739; UV/

vis (CH_3CN) λ_{max} [nm] (log ϵ) 227 (3.801), 291 (3.569), 342 (2.956); ^{1}H NMR (600 MHz, CD_3CN) δ 2.78−2.91 (m, 16 H, CH_2−cyclen), 2.94−2.97 (m, 4 H, CH_2−cyclen), 3.01−3.05 (m, 4 H, CH_2−cyclen), 3.08−3.11 (m, 2 H, NH), 3.17−3.21 (m, 4 H, CH_2−cyclen), 3.32−3.36 (m, CH_2−cyclen), 3.53−3.58 (m, 4 H, NH), 7.67 (d, 2 H, ^3J = 8.04 Hz, CH−pyridine), 8.06 (d, 2 H, ^3J = 7.65 Hz, CH−pyridine), 8.17 (dd, 2 H, ^3J = 8.04 and 7.65 Hz, CH−pyridine); ^{13}C NMR (150 MHz, CD_3CN) δ 44.3 (−, CH_2−cyclen), 44.9 (−, CH_2−cyclen), 45.8 (−, CH_2−cyclen), 53.5 (−, CH_2−cyclen), 119.7 (+, C_{aryl}−H−pyridine), 122.9 (+, C_{aryl}−H−pyridine), 142.9 (+, C_{aryl}−H−pyridine), 154.8 (C_{quat}, C_{aryl}−N−pyridine), 162.7 (C_{quat}, C_{aryl}−N−pyridine); MS (ESI, CH_3CN/H_2O) *m/z* (%) 241 (100) $[M^{4+} + ClO_4^-]^{3+}$, 228 (70) $[M^{4+} + CH_3COO^-]^{3+}$, 370 (50) $[M^{4+} + ClO_4^- + OH^-]^{2+}$; MS (ESI, negative, CH_3CN/H_2O) *m/z* (%) 1041 (100) $[M^{4+} + 4ClO_4^- + OH^-]^-$. Anal. Calcd for $C_{26}H_{44}N_{10}O_{16}Cl_4Zn_2 \cdot H_2O$: C, 29.93; H, 4.44; N, 13.43. Found: C, 29.81; H, 4.21; N, 13.11.

6,6″-Bis(1,4,7-tris-*tert*-butyloxycarbonyl)-1,4,7,10-tetraazacyclododecane-2,2′:6′,2″-terpyridine (16). Compound **16** was prepared according to procedure B described in the literature.[21] A mixture of 1,4,7,10-tetraazacyclododecane-1,4,7-tricarboxylic acid tri-*tert*-butyl ester (1.90 g, 4.03 mmol) and 6,6″-dibromo-2,2′:6′,2″-terpyridine (0.75 g, 1.92 mmol) was treated with sodium *tert*-butylate. $Pd(OAc)_2/PPh_3$ was used as the catalyst. The reaction mixture was heated for 34 h at 80 °C and then purified by column chromatography on silica. Compound **16** (R_f = 0.11, ethyl acetate/petroleum ether, 3:7) was isolated as the main product. Yield: 1.54 g (68%, 81% corrected yield according to the starting material conversion). The dehydrohalogenation product (0.125 g, 9%, 11% corrected yield according to the starting material conversion; R_f = 0.19, EE/PE, 3:7) was isolated as a side product. The homoaryl coupling product was not formed in a significant amount and was only observed by mass spectroscopy in the raw reaction mixture: MS (ESI, CH_2Cl_2/MeOH + 1% AcOH) *m/z* (%) 1406 (9) $[MH]^+$; mp 127 °C; IR (KBr) $\tilde{\nu}$ [cm^{-1}] 2974, 2930, 1703, 1568, 1412, 1250, 1171, 860, 778, 633; UV/vis (CH_3CN) λ_{max} [nm] (log ϵ) 226 (3.592), 271 (3.429), 350 (2.984); ^{1}H NMR (600 MHz, $CDCl_3$) δ 1.45 (s, 54 H, CH_3−Boc), 3.25−3.78 (m, 32 H, CH_2−cyclen), 6.64 (d, 2 H, ^3J = 8.3 Hz, CH−pyridine), 7.61 (dd, 2 H, ^3J = 8.3 and 7.4 Hz, CH−pyridine), 7.86 (t, 1 H, ^3J = 7.8 Hz, CH *8*), 7.97 (d, 2 H, ^3J = 7.4 Hz, CH−pyridine), 8.30 (d, 2 H, ^3J = 7.8 Hz, CH−pyridine); ^{13}C NMR (150 MHz, $CDCl_3$) δ 28.4, 28.5 (+, CH_3−Boc), 50.3, 50.7, 52.2 (−, CH_2−cyclen), 79.9, 80.2 (C_{quat}, C−Boc), 108.0 (+, C_{aryl}−H−pyridine), 110.1 (+, C_{aryl}−H−pyridine), 120.1 (+, C_{aryl}−H−pyridine), 137.4 (+, C_{aryl}−H−pyridine), 138.1 (+, C_{aryl}−H−pyridine), 154.0, 155.8 (C_{quat}, C_{aryl}−N−pyridine), 156.4 (C_{quat}, C═O−Boc), 159.1 (C_{quat}, C_{aryl}−N−pyridine); MS (ESI, CH_2Cl_2/MeOH + 10 mmol/L of NH_4Ac) *m/z* (%) 1175 (100) $[MH]^+$, 588 (20) $[M + 2H]^{2+}$, 1197 (10) $[M + Na]^+$. Anal. Calcd for $C_{61}H_{95}N_{11}O_{12}$: C, 62.37; H, 8.16; N, 13.12. Found: C, 62.05; H, 8.15; N, 12.58.

6,6″-Bis(10-aza-1,4,7-triazoniacyclododecan-10-yl)-2,2′:6′,2″-terpyridine Hexakis(trifluoroacetate) (17). A procedure analogous to that described for **3** was followed starting from a solution of **16** (0.90 g, 0.77 mmol) in dichloromethane (40 mL) and TFA (3.5 mL, 5.18 g, 45.44 mmol). After the addition of TFA, the color of the solution turned intensively yellow. The salt **17** was isolated quantitatively as a yellow, very viscous oil, in quantitative yield: IR (KBr) $\tilde{\nu}$ [cm^{-1}] 3445, 2991, 2889, 1679, 1610, 1202, 1136, 866, 789, 718; UV/vis (CH_3CN) λ_{max} [nm] (log ϵ) 224 (3.738), 261 (3.504), 334 (3.210); ^{1}H NMR (300 MHz, CD_3CN) δ 3.12−3.14 (m, 8 H, CH_2−cyclen), 3.20−3.26 (m, 16 H, CH_2−cyclen), 3.89−3.92 (m, 8 H, CH_2−cyclen), 7.06 (d, 2 H, ^3J = 8.7 Hz, CH), 7.71 (d, 2 H, ^3J = 7.4 Hz, CH), 7.86−7.99 (m, 3 H, CH), 8.28 (bs, 12 H, NH_2^+), 8.45 (d, 2 H, ^3J = 7.9 Hz, CH); ^{13}C NMR (75 MHz, CD_3CN) δ 45.4, 45.6, 47.3, 50.2 (−, CH_2−cyclen), 112.9, 113.6 (+, C_{aryl}−H), 117.0 (C_{quat}, q, $^1J_{C,F}$ = 287.5 Hz, CF_3COO^-), 124.5, 141.4, 145.5 (+, C_{aryl}−H), 146.9, 150.9, 158.5 (C_{quat}, C_{aryl}−N), 160.8 (C_{quat}, q, $^2J_{C,F}$ = 36.9 Hz, CF_3COO^-); MS (ESI, MeOH + 10 mmol/L of NH_4Ac) *m/z* (%) 574 (40) $[M^{6+} - 5H]^+$, 288 (100) $[M^{6+} - 4H]^{2+}$.

6,6″-Bis(1,4,7,10-tetraazacyclododecan-1-yl)-2,2′;6′,2″-terpyridine (L7). A procedure analogous to that described for **L1** was followed. A solution of **17** (0.706 g, 0.56 mmol) in water (20 mL) was slowly passed through a column of basic ion-exchange resin (35 mL). The free amine **L7** was obtained as a pale-yellow solid: yield 0.311 g (97%); mp 98−100 °C; IR (KBr) $\tilde{\nu}$ [cm^{-1}] 3448, 2925, 2854, 1621, 1568, 1428, 1365, 787; UV/vis (CH_3CN) λ_{max} [nm] (log ϵ) 226 (4.082), 270 (3.910), 349 (3.475); ^{1}H NMR (300 MHz, MeOH-d_4) δ 2.68−2.71 (m, 8 H, CH_2−cyclen), 2.75−2.79 (m, 8 H, CH_2−cyclen), 3.03−3.11 (m, 8 H, CH_2−cyclen), 3.71−3.79 (m, 8 H, CH_2−cyclen), 6.89 (d, 2 H, ^3J = 8.4 Hz, CH−pyridine), 7.72 (dd, 2H, ^3J = 8.4 and 7.4 Hz, CH−pyridine), 7.94−8.02 (m, 3 H, CH−pyridine), 8.39 (d, 2 H, ^3J = 7.8 Hz, CH−pyridine); ^{13}C NMR (75 MHz, MeOH-d_4) δ 45.2, 47.0, 48.1, 49.9 (−, CH_2−cyclen), 108.2 (+, C_{aryl}−H−pyridine), 110.1 (+, C_{aryl}−H−pyridine), 120.0 (+, C_{aryl}−H−pyridine), 137.2 (+, C_{aryl}−H−pyridine), 137.9 (+, C_{aryl}−H−pyridine), 153.5, 155.6 (C_{quat}, C_{aryl}−N−pyridine), 158.9 (C_{quat}, C_{aryl}−N−pyridine); MS (ESI, MeOH + 10 mmol/L of NH_4Ac) *m/z* (%) 574 (100) $[MH]^+$, 288 (60) $[M + 2H]^{2+}$. HRMS ($C_{31}H_{48}N_{11}$): calcd, 574.4094 $[MH]^+$; obsd, 574.4096 $[MH]^+$ ±1.27 ppm.

$[Zn_2L7](ClO_4)_4 \cdot CH_3CN$. A procedure analogous to that described for **Zn_2L2** was followed. To a solution of **L7** (0.214 g, 0.37 mmol) in methanol (20 mL) were added slowly under intense stirring portions of a solution of $Zn(ClO_4)_2 \cdot 6H_2O$ (0.28 g, 0.74 mmol) in methanol (15 mL). A colorless precipitate immediately appeared. The mixture was stirred for 21 h at room temperature and then refluxed for 2 h. The solvent was removed under vacuum. Pale-yellow crystals were obtained after recrystallization from a mixture of MeOH/CH_3CN and 0.1 N HCl (2:4:1): yield 0.29 g (71%); mp 232 °C; IR (KBr) $\tilde{\nu}$ [cm^{-1}] 3429, 2965, 2891, 1652, 1570, 1467, 1365, 791; UV/vis (CH_3CN) λ_{max} [nm] (log ϵ) 224 (4.005), 265 (3.742), 343 (3.198); ^{1}H NMR (300 MHz, CD_3CN) δ 2.70−2.78 (m, 4 H, CH_2−cyclen), 2.86−2.98 (m, 16 H, CH_2−cyclen), 3.19−3.25 (m, 8 H, CH_2−cyclen), 3.38−3.42 (m, 2 H, NH), 3.74−3.85 (m, 8 H, CH_2−cyclen and NH), 7.34 (d, 2 H, ^3J = 8.1 Hz, CH), 7.89−8.09 (m, 3 H, CH), 8.37−8.43 (m, 4 H, CH); ^{13}C NMR (75 MHz, CH_3CN) δ 44.6, 44.8, 46.2, 52.5 (−, CH_2−cyclen), 117.8, 118.9, 123.0, 139.7, 141.1 (+, C_{aryl}−H), 155.6, 156.8, 160.5 (C_{quat}, C_{aryl}−N); MS (ESI, MeOH/CH_3CN) *m/z* (%) 410 (100) $[M^{4+} + 2CH_3COO^-]^{2+}$, 450 (40) $[M^{4+} + 2ClO_4^-]^{2+}$. Anal. Calcd for $C_{31}H_{47}N_{11}O_{16}Cl_4Zn_2 \cdot CH_3CN$: C, 34.67; H, 4.41; N, 14.70. Found: C, 34.71; H, 4.49; N, 14.92.

10-(2-Pyridinyl)-10-aza-1,4,7-triazoniacyclododecane Tris(trifluoroacetate) (19). A procedure analogous to that described for **3** was followed starting from a solution of **18**[21] (1 g, 1.82 mmol) in dichloromethane (35 mL) and TFA (4.2 mL, 6.22 g, 54.53 mmol). The product **19** was obtained quantitatively as a pale-yellow, viscous oil: mp 198−201 °C; IR (KBr) $\tilde{\nu}$ [cm^{-1}] 3421, 2951, 1630, 1538, 1484, 1284, 1095, 774; UV/vis (CH_3CN) λ_{max} [nm] (log ϵ) 249 (4.012), 304 (3.401); ^{1}H NMR (250 MHz, D_2O) δ 3.09−3.15 (m, 8 H, CH_2−cyclen), 3.29−3.39 (m, 4 H, CH_2−cyclen), 3.82−3.86 (m, 4 H, CH_2−cyclen), 6.99 (dd, 1 H, ^3J = 7.0 and 7.2 Hz, CH−pyridine), 7.16 (d, 1 H, ^3J = 9.3 Hz, CH−pyridine), 7.88 (m, 1 H, CH−pyridine), 8.01 (m, 1 H, CH−pyridine); ^{1}H NMR (600 MHz,

CD_3CN) δ 3.19−3.21 (m, 8 H, CH_2−cyclen), 3.34−3.36 (m, 4 H, CH_2−cyclen), 3.89−3.90 (m, CH_2−cyclen), 7.09 (dd, 1 H, ^3J = 7.13 and 6.31 Hz, CH−pyridine), 7.18 (d, 1 H, ^3J = 9.26 Hz, CH−pyridine), 8.03 (dd, 1 H, ^3J = 6.31 Hz, ^4J = 1.78 Hz, CH−pyridine), 8.08 (ddd, 1 H, ^3J = 9.26 and 7.13 Hz, ^4J = 1.78 Hz, CH−pyridine); ^{13}C NMR (63 MHz, D_2O) δ = 44.3, 44.6, 45.7, 49.9 (−, CH_2−cyclen), 112.9, 114.3 (+, C_{aryl}−H), 116.2 (C_{quart}, q, $^1J_{C,F}$ = 292.4 Hz, CF_3COO^-), 136.6, 145.2 (+, C_{aryl}−H), 152.1 (C_{quart}, C_{aryl}−N), 162.8 (C_{quart}, q, $^2J_{C,F}$ = 36.1 Hz, CF_3COO^-); ^{13}C NMR (150 MHz, CD_3CN) δ 44.3, 44.9, 45.5, 50.1 (−, CH_2−cyclen), 112.8 (+, C_{aryl}−H−pyridine), 113.9 (+, C_{aryl}−H−pyridine), 116.5 (C_{quart}, q, $^1J_{C,F}$ = 291.9 Hz, CF_3COO^-), 136.9 (+, C_{aryl}−H−pyridine), 144.6 (+, C_{aryl}−H *3*), 152.5 (C_{quart}, C_{aryl}−N−pyridine), 159.3 (C_{quart}, q, $^2J_{C,F}$ = 36.4 Hz, CF_3COO^-); MS (ESI, CH_3CN) *m*/*z* (%) 250 (100) $[M^{3+} - 2H]^+$.

1-(2-Pyridinyl)-1,4,7,10-tetraazacyclododecane (L8). A procedure analogous to that described for **L1** was followed. A solution of **19** (0.8 g, 1.35 mmol) in water (20 mL) was slowly passed through a column of basic ion-exchange resin (45 mL). The free amine **L8** was obtained as colorless solid: yield 0.32 g (95%); mp 89 °C; IR (KBr) $\tilde{\nu}$ [cm^{-1}] 3410, 2927, 2831, 1628, 1558, 1360, 1283, 770, 599; UV/vis (CH_3CN) λ_{max} [nm] (log ϵ) 251 (4.134), 309 (3.638); ^{1}H NMR (300 MHz, MeOH-d_4) δ 2.56−2.65 (m, 4 H, CH_2−cyclen), 2.71−2.79 (m, 4 H, CH_2−cyclen), 2.87−2.94 (m, 4 H, CH_2−cyclen), 3.62−3.66 (m, 4 H, CH_2−cyclen), 6.62−6.67 (m, 1 H, CH−pyridine), 6.83 (d, 1 H, ^3J = 8.7 Hz, CH−pyridine), 7.51−7.55 (m, 1 H, CH−pyridine), 8.06−8.10 (dd, 1 H, ^3J = 6.7 Hz, ^4J = 1.9 Hz, CH−pyridine); ^{13}C NMR (75 MHz, MeOH-d_4) δ 46.7, 48.4, 49.1, 51.2 (−, CH_2−cyclen), 109.8, 114.4, 138.7, 148.4 (+, C_{aryl}−H), 161.0 (C_{quart}, C_{aryl}−N); MS (ESI, CH_2Cl_2/MeOH + 10 mmol/L of NH_4Ac) *m*/*z* (%) 250 (100) $[MH]^+$. Anal. Calcd for $C_{13}H_{23}N_5$: C, 62.62; H, 9.30; N, 28.09. Found C, 62.43; H, 9.11; N, 27.72.

[ZnL8](ClO$_4$)$_2$. A procedure analogous to that described for **ZnL1** was followed. To a solution of **L8** (0.2 g, 0.80 mmol) in methanol (15 mL) were added under intense stirring portions of a solution of $Zn(ClO_4)_2 \cdot 6H_2O$ (0.298 g, 0.80 mmol) in methanol (5 mL). The mixture was refluxed for 15 h. After removal of the solvent under vacuum, the residue was recrystallized from a mixture of MeOH/H_2O (3:1). The product was isolated as colorless crystals: yield 0.409 g (95%); mp 234 °C; IR (KBr) $\tilde{\nu}$ [cm^{-1}] 3214, 2920, 2872, 1588, 1383, 1285, 780, 592; UV/vis (CH_3CN) λ_{max} [nm] (log ϵ) 250 (4.007), 305 (3.509); ^{1}H NMR (300 MHz, MeOH-d_4) δ 2.50−2.62 (m, 2 H, CH_2−cyclen), 2.81−2.94 (m, 6 H, CH_2−cyclen), 2.99−3.09 (m, 4 H, CH_2−cyclen), 3.35−3.44 (m, 4 H, CH_2−cyclen), 7.61−7.66 (m, 1 H, CH−pyridine), 7.78 (d, 1 H, ^3J = 8.2 Hz, CH−pyridine), 8.18−8.25 (m, 1 H, CH−pyridine), 8.49 (dd, 1 H, ^3J = 7.8 Hz, ^4J = 1.8 Hz, CH−pyridine); ^{13}C NMR (75 MHz, MeOH-d_4) δ 46.4, 46.5, 46.8, 53.1 (−, CH_2−cyclen), 121.6, 126.5, 144.7, 149.2 (+, C_{aryl}−H), 160.1 (C_{quart}, C_{aryl}−N); MS (ESI, MeOH/CH_2Cl_2 + 10 mmol/L of NH_4Ac) *m*/*z* (%) 372 (100) $[M^{2+} + CH_3COO^-]^+$, 412 (35) $[M^{2+} + ClO_4^-]^+$.

Crystallographic Study. Colorless monoclinic crystals of [**Zn$_2$L2**]μ-OH(ClO$_4$)$_3$·CH_3CN·H_2O (0.20 × 0.12 × 0.06 mm) were used for data collection at 173 (±1) K with graphite-monochromated Mo Kα radiation (λ = 0.710 73 Å) on a STOE-IPDS diffractometer. The structure of the compound [**Zn$_2$L2**]μ-OH(ClO$_4$)$_3$·CH_3CN·H_2O was solved by direct methods SIR97 and refined by full-matrix least squares on F^2 using *SHELXL-97*. The molecular structure is illustrated in Figure 1 by an ORTEP drawing with 50% probability thermal ellipsoids. Selected interatomic distances and bond angles around the Zn(II) are presented in Table 1. Crystal data and data collection parameters, atomic positional parameters with standard deviations, bond lengths, and bond angles are given as the Supporting Information.

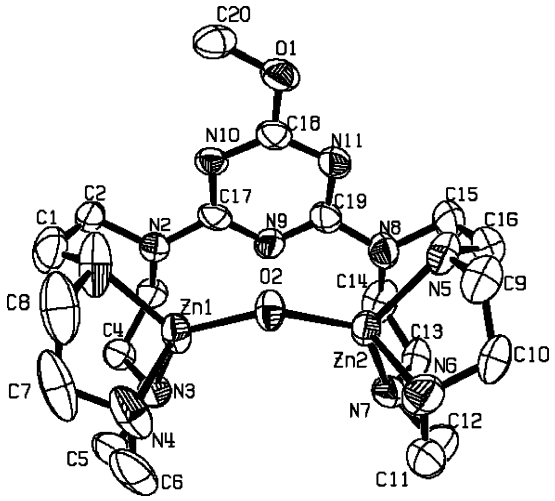

Figure 1. ORTEP drawing (50% probability ellipsoids) of [**Zn$_2$L2**]μ-OH(ClO$_4$)$_3$·CH_3CN·H_2O. All H atoms, three perchlorate anions, an acetonitrile atom, and a water molecule are omitted for clarity.

Table 1. Deprotonation Constants (pK_a) of Metal-Bound Water at 25 °C and I = 0.10 (TEAP)

metal complex	pK_a	metal complex	pK_a
ZnL1	8.35 ± 0.03	**ZnL3**	8.28 ± 0.05
NiL1	11.13 ± 0.02	**ZnL8**	7.89 ± 0.05
CuL1[a]		Zn[12]aneN$_4$[b]	8.06 ± 0.01

[a] Titration was not possible because of insufficient solubility. [b] This work.

Potentiometric pH Titrations. The pH titrations were carried out under nitrogen at 25 °C with a computer-controlled pH meter (pH 3000, WTW) and dosimat (Dosimat 665 and 765, Metrohm). Aqueous or methanol (water/methanol, 9:1) solutions of the metal complexes (0.1 mM for the Zn(II) complexes and 0.25 mM for the Cu(II) and Ni(II) complexes) were titrated with a 0.1 M tetraethylammonium hydroxide (TEAOH) aqueous solution. The ionic strength was adjusted to I = 0.1 with tetraethylammonium perchlorate (TEAP). The TEAOH solutions were calibrated with monosodium phthalate. A titration of 0.1 M perchloric acid with a TEAOH solution was used for calibration and to determine log K_W. For the dinuclear complexes **Zn$_2$L4** and **Zn$_2$L5**, 0.5 equiv of $HClO_4$ was added to the titration solution in order to determine values in the pH range of 5−8. The Irving factor (A_I) was determined according to $pH_{measurement} = pH_{real} + A_I$ in the corresponding solvent. For each metal complex, at least two independent titrations were made. The complex **CuL1** was not soluble enough to allow a potentiometric pH titration. Data analysis was performed with the programs *Hyperquad2000* (version 2.1, P. Gans) and *Origin 6.0*. The deprotonation constants K_a are defined as [ML-OH^-]a_{H+}/[ML].

Kinetic Measurements. The hydrolysis rate of NA promoted by ML-OH^- species was measured by an initial slope method following the increase in the 400-nm absorption of 4-nitrophenolate in a 10% (v/v) CH_3CN aqueous solution in the pH ranges of 6.5−9.5 for the Zn(II) complexes and of 7−9 for the Cu(II) and Ni(II) complexes (50 mM HEPES, Tris, or CHES buffer, I = 0.1 M, NaCl) at 25 °C. The reactions were corrected for the degree of ionization of 4-nitrophenol at the respective pH and temperature (see the Supporting Information Figure 1). The kinetic data were collected under pseudo-first-order conditions (excess of the metal complex). Using the log ϵ value of 4.26 for 4-nitrophenolate (experimentally

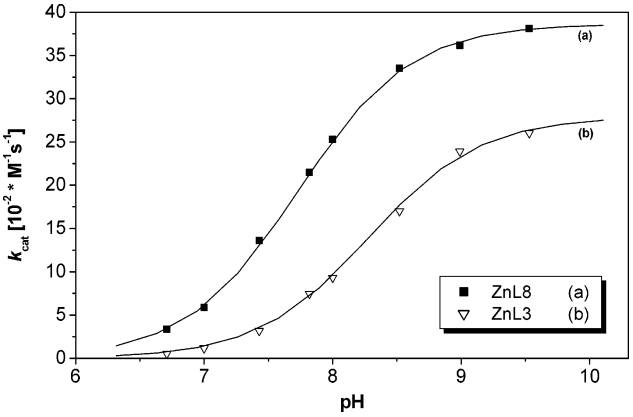

Figure 2. pH−rate profile for the second-order rate constants of NA hydrolysis of **ZnL3** and **ZnL8** at 25 °C and $I = 0.10$ (NaCl) in 10% (v/v) CH_3CN.

determined; see the Supporting Information), the initial rate of 4-nitrophenolate release was calculated, whereby three independent measurements were made. From the obtained slope ([produced 4-nitrophenolate]/time) and the concentration of NA, the pseudo-first-order rate constant k_{obs}(NA) (s^{-1}) was determined. A plot of these k_{obs} values vs metal complex concentrations at a given pH gave a straight line, with its slope representing the second-order rate constant $k_{cat.}$(NA) (M^{-1} s^{-1}). All correlation coefficients are >0.9989. Correction for the spontaneous hydrolysis of the substrate by the solvent was accomplished either by direct measurement of the difference between the production of 4-nitrophenolate in the reaction cell and a reference cell containing the same concentration of carboxyester as that in the reaction cell in the absence of the metal complex or by separate measurement of the general rate of spontaneous hydrolysis for NA (see the Supporting Information Figure 2). The determined value of 8.16 M^{-1} s^{-1} for k_{OH} (the rate constant describing the attack of free OH^- anions) matches the values obtained from the intercepts of the plots of k_{obs} vs metal complex concentrations. The reaction solutions contained 0.1−0.5 mM Cu(II), 0.0002−0.075 mM Ni(II), and 0.005−3.0 mM Zn(II) complexes, 0.003−2.0 mM NA, and 50 mM buffer. The absorption increase was recorded immediately after mixing and then monitored until 5% formation of 4-nitrophenolate.

Results and Discussion

Syntheses of the Ligands L1−L8 and Their Metal Complexes (Schemes 1−3). Ligands **L1**−**L8** were obtained by a previously developed synthetic route. The first step of the synthesis has already been disclosed for the monosubstituted compound **1**.[19] Ligand **L1** was obtained from compound **1** by nucleophilic substitution with sodium methylate, deprotection of the Boc groups with TFA, and elution from a basic ion-exchange resin with an overall yield of 98% (Scheme 1). The same procedure gave **L8** starting from the previously reported compound tri-*tert*-butyl-10-(2-pyridinyl)-1,4,7,10-tetraazacyclododecane-1,4,7-tricarboxylate (**18**).[21]

Similarly, **L3** was obtained in an overall yield >90% after coupling of the azacrown moiety to **1**, yielding **8** (Scheme 2). The ligands **L2** and **L4** were prepared starting from the previously reported compound **4**[20] using the same synthetic pathways as those for **L1** and **L3**, respectively (Scheme 3). The ligands **L5** and **L6** were obtained starting from the previously reported compounds[21] **12** and **14**. By following the same procedure[21] as that for **12** and **14**, the new compound **16** was synthesized, from which ligand **L7** was prepared (Scheme 3). Metal complexes were isolated in analytical purity with good yields (53−98%) from the reaction of the ligands with metal perchlorate salts in MeOH [for Zn(II)] or EtOH [for Ni(II) and Cu(II)] and characterized by different methods (^1H and ^{13}C NMR, UV/vis, IR, ESI, elemental analysis, and HRMS) to show a stoichiometry of 1:1 metal cation/ligand for mononuclear complexes and 2:1 metal cation/ligand for dinuclear complexes. In all cases, the heteroaromatic spacer is directly connected to the macrocycle, without any pendant arm,[22−24] which leads to more rigid structures.

Deprotonation Constants (pK_a) of the Metal-Bound Water. The pK_a values were determined by pH-metric titrations in aqueous or MeOH/H_2O (1:9) solutions under nitrogen at 25 °C and $I = 0.1$ (TEAP). The pH profiles and species distribution diagrams of all complexes can be found in the Supporting Information. The pK_a values of the mononuclear metal complexes are summarized in Table 1.

CuL1 was not sufficiently soluble under the given experimental conditions to allow a potentiometric pH titration. However, its UV and IR spectra indicate a square-pyramidal complex with one molecule of water as the fifth ligand, as reported in the literature.[25] The UV and IR spectra of **NiL1** coincide also with the usual structure of Ni[12]aneN$_4$ complexes, reported to have a high-spin cis-octahedral geometry with two coordinated water molecules,[26] with the pK_a value of the second water molecule being higher than pH 13. Among the mononuclear Zn complexes, **ZnL8** shows the smallest pK_a value.

For the dinuclear complexes **Zn_2L4** (in an aqueous solution) and **Zn_2L5** [in a MeOH/H_2O (9:1) solution], two distinct buffer regions were determined, one around pH 6 and the other in the pH range of 8−10, corresponding to three distinct pK_a values. The model curve fitted to the pH titration profiles corresponds to three pK_a values with complete deprotonation after the addition of 2 equiv of the base. The titration curves of **Zn_2L2** [in an aqueous solution and in a MeOH/H_2O (9:1) solution] show only one deprotonation constant in the pH range of 9 but have a high similarity to the upper part of the titration curves of **Zn_2L4** and **Zn_2L5**. This observation is rationalized by the low solubility of **Zn_2L2**, which did not allow an exact determi-

(22) (a) Raidt, M.; Neuburger, M.; Kaden, T. A. *Dalton Trans.* **2003**, 1292. (b) Kaden, T. A. *Coord. Chem. Rev.* **1999**, *190*−*192*, 371.
(23) (a) Vichard, C.; Kaden, T. A. *Inorg. Chim. Acta* **2002**, *337*, 173. (b) Vichard, C.; Kaden, T. A. *Inorg. Chim. Acta* **2004**, *357*, 2285.
(24) (a) Arca, M.; Bencini, A.; Berni, E.; Caltagirone, C.; Devillanova, F. A.; Isaia, F.; Garau, A.; Giorgi, C.; Lippolis, V.; Pera, A.; Tei, L.; Valtancoli, B. *Inorg. Chem.* **2003**, *42*, 6929. (b) Iranzo, O.; Elmer, T.; Richard, J. P.; Morrow, J. R. *Inorg. Chem.* **2003**, *42*, 7737.
(25) (a) Styka, M. C.; Smierciak, R. C.; Blinn, E. L.; DeSimone, R. E.; Passariello, J. V. *Inorg. Chem.* **1978**, *17*, 82. (b) Thöm, V. J.; Hosken, G. D.; Hancock, R. D. *Inorg. Chem.* **1985**, *24*, 3378.
(26) (a) Fabrizzi, L.; Micheloni, M.; Paoletti, P. *Inorg. Chem.* **1980**, *19*, 535. (b) Fabrizzi, L. *Inorg. Chem.* **1977**, *16*, 2667. (c) Bencini, A.; Bianchi, A.; Garcia-Espana, E.; Jeannin, Y.; Julve, M.; Marcelino, V.; Philoche-Levisalles, M. *Inorg. Chem.* **1990**, *29*, 963.

Scheme 1. Synthesis of **L1** and the Corresponding Metal Complexes

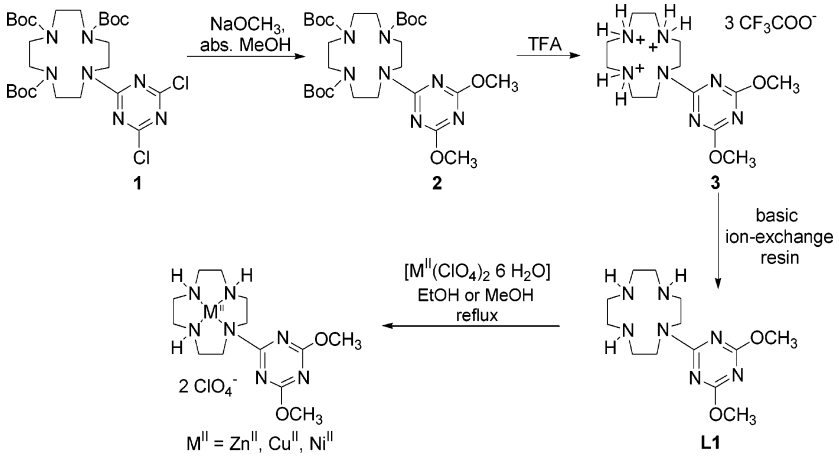

Scheme 2. Synthesis of **L3** and the Corresponding Metal Complex

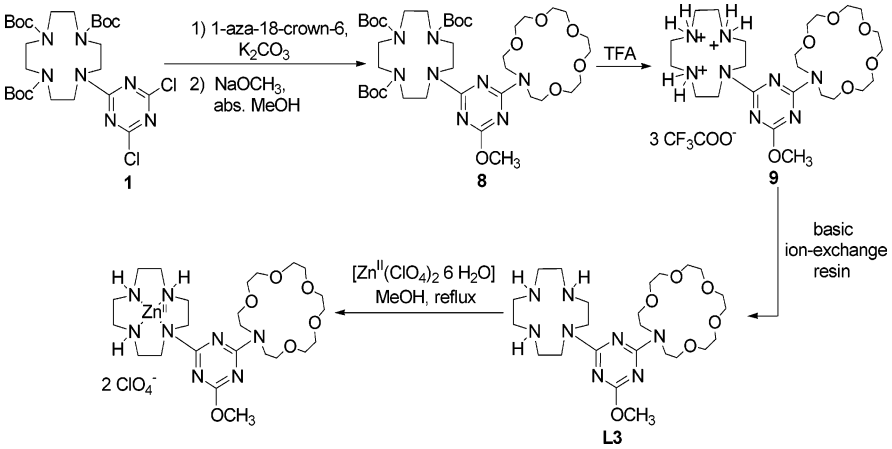

nation of the buffer curve at lower pH range. Titration with a more diluted base (0.025 M instead of 0.1 M) did not improve the measurement. **Zn_2L2** is supposed to have three pK_a values, but for the chosen experimental conditions, only one of them could be determined. The proposed chemical model for the deprotonation steps of **Zn_2L4**, **Zn_2L5**, and **Zn_2L2** is shown in Scheme 4. The model is based on an equilibrium in solution between the μ-hydroxo-bridged species **Zn_2L**(μ-OH_2)(OH_2), analogous to the obtained crystal structure, and an open form corresponding to the species where each Zn(II) ion is coordinating to a water molecule, **Zn_2L**(OH_2)$_2$. This model is supported by a good match of the calculated and measured pH profiles and reports from the literature, where a similar equilibrium between open and closed species was postulated.[27] The proton-independent equilibrium K_{D1} can be determined indirectly. The pK_a values of **Zn_2L2, Zn_2L4**, and **Zn_2L5** are summarized in Table 2. Alternative models with two deprotonation steps, either consecutive or independent from one another, or a model with the dinuclear metal complex coordinating to three water molecules, one at each metal ion and one as a μ-hydroxo bridge, as observed for the crystal structure of **Zn_2L2** and reported for other macrocyclic Zn complexes,[28] do not fit the experimental data.

The pK_a value of the μ-hydroxo-coordinated water molecule, pK_{a3}, is smaller than those reported for similar compounds,[27c] indicating an enhanced acidity and stability of the μ-hydroxo bridge due to the close proximity of the two zinc(II) cyclen moieties.

For the remaining dinuclear complexes, **Cu_2L2**, **Ni_2L2**, **Zn_2L6**, and **Zn_2L7**, the pH profiles correspond to those of the general model,[29] with each metal ion coordinating to a water molecule and two successive deprotonation steps leading to the species $M_2L(OH^-)_2$ (Scheme 5).

The pK_a values of these complexes are summarized in Table 3.

The pH profile of **Cu_2L2**, together with its UV and IR spectra, indicates the structure of the complex, with each copper cyclen unit possessing the already reported square-pyramidal geometry[25] and with each Cu(II) ion coordinating to the four N atoms of the macrocycle and one water molecule. Therefore, there is neither a μ-hydroxo bridge

(27) (a) Fujioka, H.; Koike, T.; Yamada, N.; Kimura, E. *Heterocycles* **1996**, *42*, 775. (b) Koike, T.; Takashige, M.; Kimura, E.; Fujioka, H.; Shiro, M. *Chem.—Eur. J.* **1996**, *2*, 617. (c) Kimura, E.; Aoki, S.; Koike, T.; Shiro, M. *J. Am. Chem. Soc.* **1997**, *119*, 3068. (d) Aoki, S.; Kimura, E. *J. Am. Chem. Soc.* **2000**, *122*, 4542.

(28) (a) Yashiro, M.; Kaneiwa, H.; Onaka, K.; Komiyama, M. *J. Chem. Soc., Dalton Trans.* **2004**, 605. (b) Kinoshita, E.; Takahashi, M.; Takeda, H.; Shiro, M.; Koike, T. *J. Chem. Soc., Dalton Trans.* **2004**, 1189.

(29) (a) Yoo, C. E.; Chae, P. S.; Kim, J. E.; Jeong, E. J.; Suh, J. *J. Am. Chem. Soc.* **2003**, *125*, 14580. (b) Aoki, S.; Kimura, E. *Rev. Mol. Biotechnol.* **2002**, *90*, 129 and references cited therein.

Scheme 3. Synthesis of **L2**, **L4**−**L7**, and Their Metal Complexes

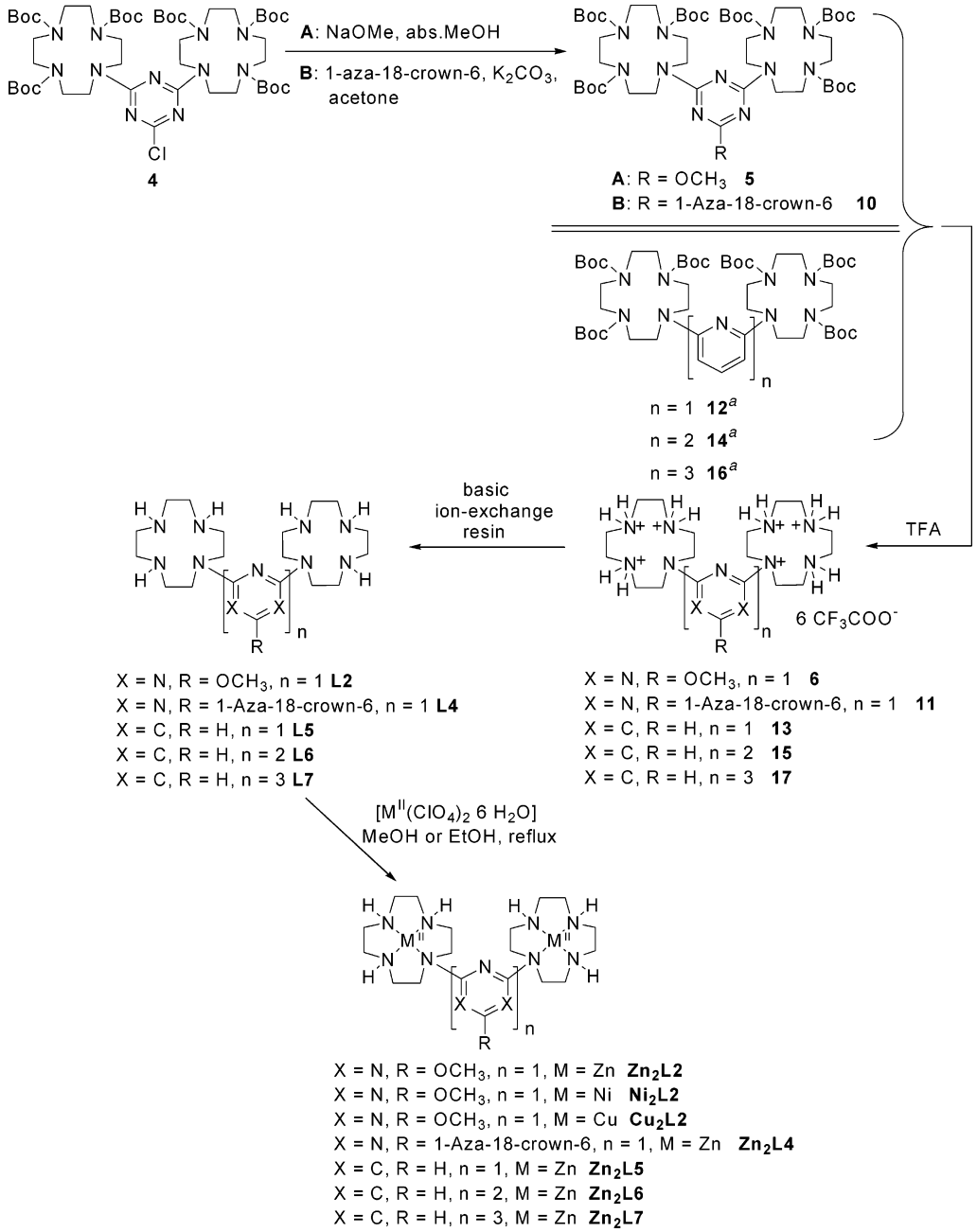

[a] For synthesis and characterization of these previously published compounds, see the Experimental Section.

present between the two metal centers, as in the case of **Zn_2L2** or as reported in the literature for Cu[9]aneN_3 complexes,[10a,c,30] nor any coordination of the Cu(II) ions to the N atom of the bridging hetarene, as observed in a pyridyl-bridged copper(II) bis(cyclen) complex.[31]

The successive deprotonation of the water molecules indicates an interaction between the two metal centers. The strength of this interaction is influenced by the spacer length,[24b,32] as observed from the differences between the two pK_a values: a shorter spacer length leads to stronger interactions between the metal ions, making the second deprotonation step more difficult and thus increasing the difference between the two pK_a values. For **Zn_2L6** with the shorter diaryl spacer, this difference is $\Delta pK_a = 1.4$, while for **Zn_2L7** with the longest spacer, it is only $\Delta pK_a = 0.5$. Compound **Zn_2L5** possessing a short aryl spacer was shown to form a μ-hydroxo bridge between the two metal centers. For the Ni(II) and Cu(II) complexes, the small difference between the pK_a values indicates a very weak interaction between the two metal ions.

X-ray Crystal Structure of the Complex [Zn_2L2]μ-OH-$(ClO_4)_3$·CH_3CN·H_2O. A solution of [**Zn_2L2**]$(ClO_4)_4$·

(30) Belousoff, M. J.; Duriska, M. B.; Graham, B.; Batten, S. R.; Moubaraki, B.; Murray, K. S.; Spiccia, L. *Inorg. Chem.* **2006**, *45*, 3746.

(31) El Ghachtouli, S. E.; Cadiou, C.; Deschamps-Olivier, I.; Chuburu, F.; Aplincourt, M.; Turcry, V.; Le Baccon, M.; Handel, H. *Eur. J. Inorg. Chem.* **2005**, 2658.

(32) McCue, K. P.; Morrow, J. *Inorg. Chem.* **1999**, *38*, 6136.

Scheme 4. Proposed Model for the Deprotonation Steps of $\mathbf{Zn_2L4}$, $\mathbf{Zn_2L5}$, and $\mathbf{Zn_2L2}$

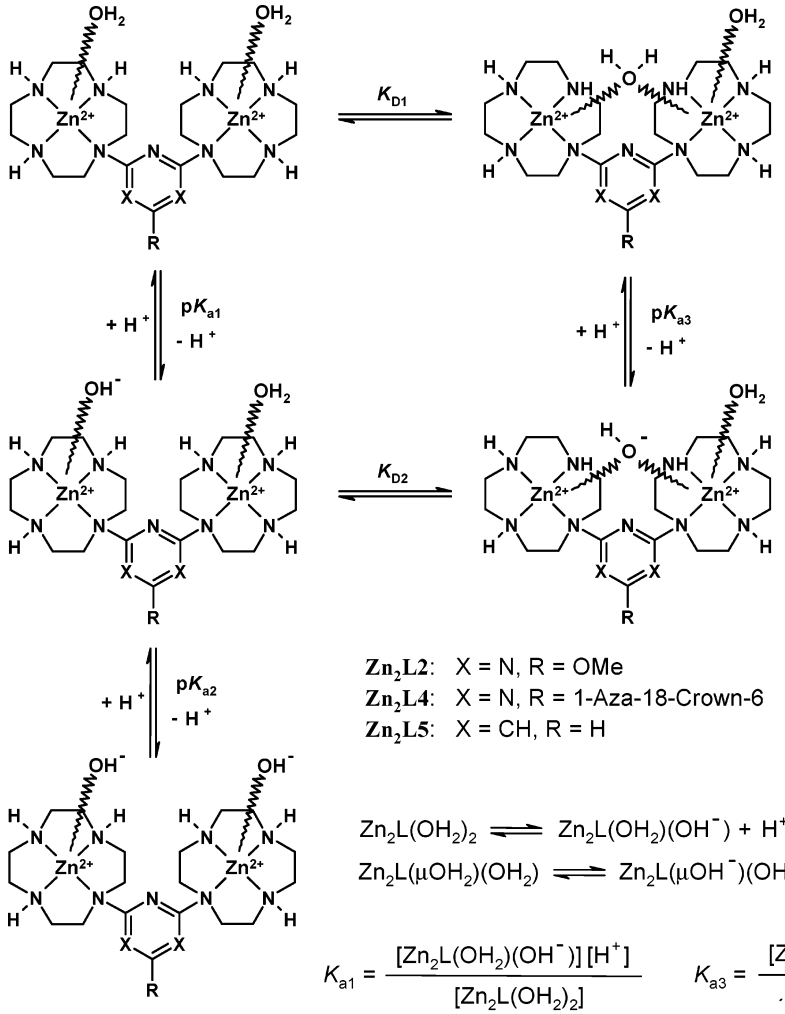

$\mathbf{Zn_2L2}$: X = N, R = OMe
$\mathbf{Zn_2L4}$: X = N, R = 1-Aza-18-Crown-6
$\mathbf{Zn_2L5}$: X = CH, R = H

$$Zn_2L(OH_2)_2 \rightleftharpoons Zn_2L(OH_2)(OH^-) + H^+$$

$$Zn_2L(\mu OH_2)(OH_2) \rightleftharpoons Zn_2L(\mu OH^-)(OH_2) + H^+$$

$$K_{a1} = \frac{[Zn_2L(OH_2)(OH^-)]\,[H^+]}{[Zn_2L(OH_2)_2]} \qquad K_{a3} = \frac{[Zn_2L(\mu OH^-)(OH_2)]\,[H^+]}{[Zn_2L(\mu OH_2)(OH_2)]}$$

$$Zn_2L(\mu OH^-)(OH_2) \rightleftharpoons Zn_2L(\mu OH^-)(OH^-) + H^+$$

$$Zn_2L(OH_2)(OH^-)_{total} \rightleftharpoons Zn_2L(OH^-)(OH^-)_{2\,total} + H^+$$

$$Zn_2L(OH_2)(OH^-)_{total} = Zn_2L(\mu OH^-)(OH_2) + Zn_2L(OH_2)(OH^-)$$

$$Zn_2L(OH^-)(OH^-)_{2\,total} = Zn_2L(\mu OH^-)(OH^-) + Zn_2L(OH^-)_2$$

$$K_{a2} = \frac{[Zn_2L(\mu OH^-)(OH^-)]\,[H^+]}{[Zn_2L(\mu OH^-)(OH_2)]} = \frac{[Zn_2L(OH^-)(OH^-)_{2\,total}]\,[H^+]}{[Zn_2L(OH_2)(OH^-)_{total}]}$$

$$Zn_2L(OH_2)_2 \rightleftharpoons Zn_2L(\mu OH_2)(OH_2) \qquad K_{D1} = \frac{[Zn_2L(\mu OH_2)(OH_2)]}{[Zn_2L(OH_2)_2]}$$

Table 2. Deprotonation Constants (pK_a) of Metal-Bound Water at 25 °C and $I = 0.10$ (TEAP)

	pK_a			
metal complex	pK_{a1}	pK_{a2}	pK_{a3}	log K_{D1}
$\mathbf{Zn_2L2}$		9.72 ± 0.03[a]		
$\mathbf{Zn_2L4}$	8.27 ± 0.02	9.42 ± 0.06	5.96 ± 0.02	0.47 ± 0.04
$\mathbf{Zn_2L5}$	8.14 ± 0.03	9.27 ± 0.05	5.85 ± 0.02	0.64 ± 0.04

[a] The titration curve does not permit a determination of pK_{a1} and pK_{a3} values because of the insufficient solubility of the complex in water and/or MeOH/water (9:1).

CH_3CN in acetonitrile was left to stand at room temperature. After 2 weeks, colorless crystals were collected. Figure 1 shows an ORTEP drawing of the complex with 50% probability thermal ellipsoids.[33]

Selected bond lengths and bond angles around the Zn(II) ions are presented in Table 4. Crystal data and data collection parameters, atomic positional parameters with standard deviations, bond lengths, and bond angles are given as the Supporting Information.

Figure 1 shows the symmetrical structure and geometry of the Zn(II) complex. There is a OH^- bridge between the two Zn(II) ions, with equal distances Zn−O of 1.9 Å, and parallel to the plane of the triazine spacer, with a distance of 3 Å between the O atom of the bridge and N9 of triazine. Although the structure in the solid state may not coincide

(33) The experimental conditions (room temperature) cause higher vibrations of the atoms.

Scheme 5. Deprotonation Steps and Equilibrium Equations for Ni_2L2, Cu_2L2, Zn_2L6, and Zn_2L7

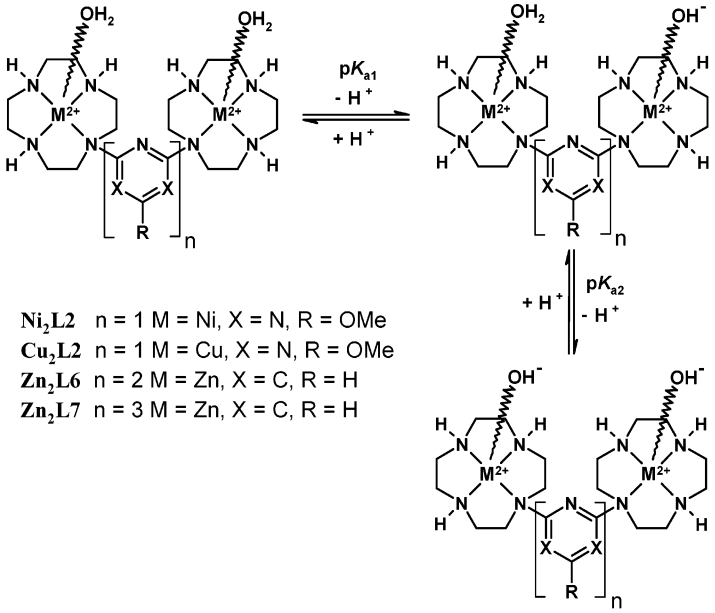

$$M_2L(OH_2)_2 \rightleftharpoons M_2L(OH_2)(OH^-) + H^+ \qquad K_{a1} = \frac{[M_2L(OH_2)(OH^-)]\ [H^+]}{[M_2L(OH_2)_2]}$$

$$M_2L(OH_2)(OH^-) \rightleftharpoons M_2L(OH^-)_2 + H^+ \qquad K_{a2} = \frac{[M_2L(OH^-)_2]\ [H^+]}{[M_2L(OH_2)(OH^-)]}$$

Table 3. Deprotonation Constants (pK_a) of Metal-Bound Water at 25 °C and $I = 0.10$ (TEAP)

metal complex	pK_{a1}	pK_{a2}
Ni_2L2	9.75 ± 0.02	10.10 ± 0.02
Cu_2L2	8.34 ± 0.03	8.68 ± 0.03
Zn_2L6	7.45 ± 0.03	8.85 ± 0.03
Zn_2L7	7.65 ± 0.01	8.11 ± 0.03

Table 4. Bond Distances, Bond Angles, and Atomic Distances for [**Zn_2L2**]μ-OH$(ClO_4)_3$·CH_3CN·H_2O[a]

Bond Distances, Å			
Zn1−O2	1.902(5)	Zn2−O2	1.909(5)
Zn1−N1	2.125(7)	Zn2−N5	2.101(6)
Zn1−N3	2.058(6)	Zn2−N6	2.074(8)
Zn1−N4	2.082(8)	Zn2−N7	2.036(6)
Bond Angles, deg			
O2−Zn1−N1	113.9(3)	O2−Zn2−N5	117.2(2)
O2−Zn1−N3	125.4(2)	O2−Zn2−N6	113.9(3)
O2−Zn1−N4	110.9(3)	O2−Zn2−N7	122.2(2)
N1−Zn1−N3	117.9(3)	N5−Zn2−N6	85.7(3)
N1−Zn1−N4	88.2(3)	N5−Zn2−N7	117.2(2)
N3−Zn1−N4	87.0(3)	N6−Zn2−N7	88.1(3)
Distances Zn1−N2, Zn2−N8, Zn1−Zn2, and O2−N9			
Zn1−N2	2.592	Zn2−N8	2.663
O2−N9	3.002	Zn1−Zn2	3.602

[a] Estimated standard deviations are in parentheses.

with the situation in the solution, it demonstrates the ability of the dinuclear complex to form an OH^- bridge, which may act as the active species in the hydrolysis of carboxyesters.

The distances between the Zn atom and three of the N atoms of cyclen are around 2.1 Å, as is generally reported for the zinc cyclen complex,[5,8,34] but the distances to the aryl-bound nitrogens N2 and N8 are each 2.6 Å, which is too long to allow a bond. This longer distance is explained by the influence of the triazine, which withdraws as an electron-poor aromatic system electron density of the cyclen N atom, thus making coordination to the metal ion by this fourth N atom less probable. Kimura et al. have shown a similar coordination pattern for two zinc cyclen complexes having dinitrobenzene[35] and pyridine[36] as cyclen pendants. Each Zn(II) ion has a distorted tetrahedral geometry, coordinating to three N atoms of cyclen and the apical O atom of the OH^- bridge. In fact, the coordination type, bond lengths, and angles (especially those for Zn1, N3, and N4 and Zn2, N6, and N7, respectively) of our complex resemble more those of a Zn[9]aneN_3[16c,37] complex, where the metal ion is coordinated by only three N atoms. The two metal ions are separated by 3.6 Å, and the electrostatic interaction between them is shielded by the ionized hydroxo bridge. This distance is in the range (3.0−4.0 Å) observed for other related alkoxo-bridged dinuclear Zn(II) complexes[17h,38] and for dinuclear Zn(II) cores of many metallohydrolases.[2c]

Hydrolysis of NA Promoted by the Mononuclear Metal Complexes. The reaction rates of ester bond cleavage of NA (0.003−2 mM) were measured by an initial slope method following the increase in the 400-nm absorption of 4-nitrophenolate in a 10% (v/v) CH_3CN aqueous solution in the

(34) Shionoya, M.; Kimura, E.; Shiro, M. *J. Am. Chem. Soc.* **1993**, *115*, 6730.
(35) Koike, T.; Gotoh, T.; Aoki, S.; Kimura, E.; Shiro, M. *Inorg. Chim. Acta* **1998**, *270*, 424.
(36) Aoki, S.; Kagata, D.; Shiro, M.; Takeda, K.; Kimura, E. *J. Am. Chem. Soc.* **2004**, *126*, 13377.
(37) Iranzo, O.; Kovalevsky, A. Y.; Morrow, J. R.; Richard, J. P. *J. Am. Chem. Soc.* **2003**, *125*, 1988.
(38) Bazzicalupi, C.; Bencini, A.; Berni, E.; Bianchi, A.; Fedi, V.; Fusi, V.; Giorgi, C.; Paoletti, P.; Valtancoli, B. *Inorg. Chem.* **1999**, *38*, 4115.

Chart 3. Structures of Previously Studied Mononuclear Zn(II) Complexes

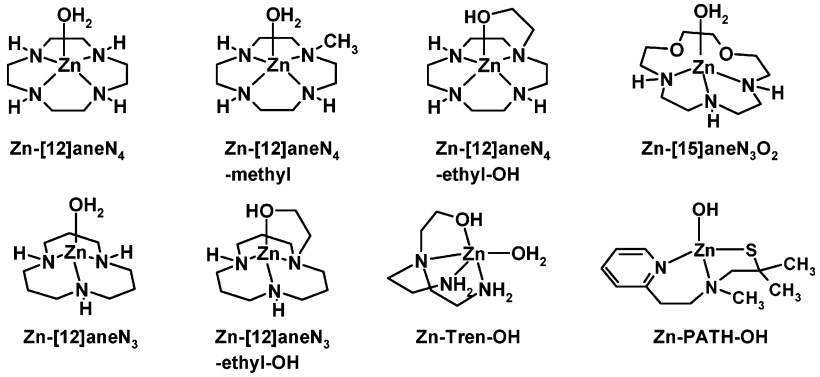

pH range of 6.5−9.5 (50 mM HEPES, Tris, or CHES buffer, $I = 0.1$ M, NaCl) at 25 °C. The reactions were corrected for the degree of ionization of 4-nitrophenol at the respective pH and temperature. The absorption increase was recorded immediately after mixing and then monitored generally until a maximum 5% formation of 4-nitrophenolate. Correction for the spontaneous hydrolysis of the substrate by the solvent was accomplished either by direct measurement of the difference between the production of 4-nitrophenolate in the reaction cell and a reference cell containing the same concentration of carboxyester as that in the reaction cell in the absence of the metal complex or by calculation of the general rate of spontaneous hydrolysis in the pH range of 7−8.5 for NA and its subtraction from the measured rate of hydrolysis. The calculation of the general rate of spontaneous hydrolysis for NA is presented in the Supporting Information. The second-order dependence of the rate constant $k_{cat.}$ on the concentration of NA and the metal complex fits the kinetic equation 1.

$$v_{cat.} = k_{cat.}[ML][NA] \quad (1)$$

In eq 1, $k_{cat.}$ is the observed NA hydrolysis rate caused by the metal complex, which was derived by subtraction of the solvent-promoted NA spontaneous hydrolysis rate from the total observed NA hydrolysis rate.

$$v = v_{cat.} + v_{\text{spontaneous hydrolysis}} = k_{obs}[NA] = (k_{cat.}[ML] + k_{OH}[OH^-] + k_0)[NA]$$

The k_{OH} value is a second-order rate constant describing the nucleophilic attack of the OH^- ions. The k_0 value is a first-order constant describing the solvolysis of the ester due to solvent molecules (e.g., water or organic additives).

The reactions were carried out under pseudo-first-order conditions with an excess of the metal complex over NA,[24b,36] where the rate constants k_{obs} (s^{-1}) were obtained by an initial slope method ([produced 4-nitrophenolate]/time) using the log ϵ values (experimentally determined; see the Supporting Information). A plot of k_{obs} vs the metal complex concentration at a given pH gave a straight line, with the slope of this line being the second-order rate constant $k_{cat.}$ (M^{-1} s^{-1}).

CuL1 showed poor solubility under the given experimental conditions and could therefore not be used for the hydrolysis experiments. A change in the solvent or an increase in the temperature would have made the measurements possible but prevents a meaningful comparison of the reactivity. **NiL1** did not show a significant effect on the hydrolysis (k_{obs} values in the range of 10^{-7}−10^{-6} s^{-1}), a fact easily explained by the percentage of active species in solution, which is on the order of 0.0069 for pH 7, 0.069 for pH 8, and 0.69 for pH 9. It is obvious that at these pH values the rate of hydrolysis is very small but at higher pH values the spontaneous hydrolysis of the substrates would be the predominant reaction taking place.

Kimura et al. have shown for the hydrolysis of NA with various Zn[12]aneN$_3$ and Zn[12]aneN$_4$ complexes that the active nucleophilic species attacking the ester is, in fact, the $ZnLOH^-$ species.[5a,9,39] The total concentration of the mononuclear metal complexes is composed of the following species, depending on the pH and the respective pK_a value:

$$[ML] = [MLOH_2] + [MLOH^-]$$

Thus, eq 1 can be written as follows:

$$v_{cat.} = k_{NA}[MLOH^-] \quad (2)$$

with

$$k_{NA} = [ML]k_{cat}/[MLOH^-]$$

By using the pH-independent second-order reaction rate constant k_{NA} (M^{-1} s^{-1}) instead of the pH-dependent second-order reaction rate constant $k_{cat.}$ (M^{-1} s^{-1}), we are able to compare the results of this work with previous works from the literature. Reciprocally, starting from the reported values of k_{NA} for other macrocyclic metal complexes, their $k_{cat.}$ values for pH 7 and 8 can be calculated. In this way, an indirect comparison between our results and those of the previous work is possible and the effect of the reaction conditions becomes observable.

The structures of the most efficient previously studied mononuclear metal complexes are depicted in Chart 3, and

(39) (a) Koike, T.; Kimura, E.; Nakamura, I.; Hashimoto, Y.; Shiro, M. *J. Am. Chem. Soc.* **1992**, *114*, 7338. (b) Koike, T.; Kimura, E. *J. Am. Chem. Soc.* **1991**, *113*, 8935. (c) Kimura, E.; Shiota, T.; Koike, T.; Shiro, M.; Kodama Shiro, M. *J. Am. Chem. Soc.* **1990**, *112*, 5805. (d) Kimura, E.; Nakamura, I.; Koike, T.; Shionoya, M.; Kodama, Y.; Ikeda, T.; Shiro, M. *J. Am. Chem. Soc.* **1994**, *116*, 4764.

Table 5. Comparison of Hydrolysis Rate Constants k_{NA} (M^{-1} s^{-1}) and $k_{cat.}$ (M^{-1} s^{-1}) for Previously Reported Mononuclear Metal Complexes

metal complex	10^2 k_{NA} (M^{-1} s^{-1})	10^2 $k_{cat.}$ (M^{-1} s^{-1}) pH 7	10^2 $k_{cat.}$ (M^{-1} s^{-1}) pH 8	reaction conditions[a]	pK_a	lit.
Zn[12]aneN$_3$	4.1			50 mM HEPES buffer, pH 8.2	7.2	38c
Zn[12]aneN$_3$	3.6 ± 0.3	1.4	3.1	20 mM CHES buffer, pH 9.3	7.2	38d
Zn[12]aneN$_3$−ethyl−OH	14 ± 1	4.0	11.2		7.4	38d
Zn[12]aneN$_4$	11 ± 2	1.1	5.6	20−50 mM CHES buffer, pH 9.2	7.9	9, 38b
Zn[12]aneN$_4$[b]	9.6 ± 0.1	1.063	5.38	50 mM Tris/HCl buffer	8.06	
Zn[12]aneN$_4$−ethyl−OH	46 ± 1	7.7	30.6	20 mM CHES buffer, pH 9.3	7.7	5a
Zn[12]aneN$_4$−methyl	4.9 ± 0.1				7.68	5a
Zn[15]aneN$_3$−O$_2$	60 ± 6			50 mM buffer, pH 7−9.5	8.8	40
Zn−Tren−OH	13 ± 1			20 mM Tris/HCl buffer, pH 8−9	7.74[c] (9.78)[d]	41
Zn−PATH−OH	89 ± 0.3			20 mM buffer, pH 7−9.5	8.05	42
CAII	250.000 ± 20.000			50 mM buffer, pH 6.8−9.6	6.8	43
His94Cys (CAII)	11.700 ± 2000				≥9.5	42

[a] At T = 25 °C and 10% CH_3CN. [b] This work. [c] pK_a value of Zn−ROH. [d] pK_a value of Zn−OH_2.

Table 6. Comparison of Hydrolysis Rate Constants $k_{cat.}$ (M^{-1} s^{-1}) and k_{NA} (M^{-1} s^{-1}) for the Mononuclear Metal Complexes at 25 °C in 10% (v/v) CH_3CN

complex[a]	10^2 $k_{cat.}$ (M^{-1} s^{-1}) pH 7	10^2 $k_{cat.}$ (M^{-1} s^{-1}) pH 8	$10^2 k_{NA}$ (M^{-1} s^{-1})
Zn[12]aneN$_4$	1.06 ± 0.03	5.38 ± 0.05	9.57 ± 0.06
ZnL1	1.68 ± 0.02	12.01 ± 0.03	39.08 ± 0.1
ZnL3	1.39 ± 0.03	9.61 ± 0.02	27.91 ± 0.02
ZnL8	6.03 ± 0.05	25.29 ± 0.03	38.63 ± 0.02

[a] Determined with [complex] = 0.01−1.3 mM and [NA] = 0.03−2 mM.

their reported second-order reaction rates $k_{cat.}$ and k_{NA} are presented in Table 5, together with the hydrolysis rate constants of two CAs.

The k_{NA} value determined by us for Zn[12]aneN$_4$ in the Tris/HCl buffer system is about 10% lower than the one determined by Kimura et al. for the CHES buffer system, which is a good agreement under the given error margins. The measured rate constant of Zn[12]aneN$_4$ will be used for further analysis.

A comparison of the hydrolysis rate constants for the new mononuclear metal complexes is presented in Table 6. The plots of k_{obs} vs the Zn(II) complex concentration are presented in the Supporting Information.

In order to get a better insight, the hydrolysis of NA promoted by **ZnL3** and **ZnL8** in the pH range of 6.5−9.5 was measured. For these experiments, the spontaneous hydrolysis of the substrate was corrected by direct measurement of the difference between the production of 4-nitrophenolate in the reaction cell and a reference cell containing only carboxyester in the same concentration as that in the reaction cell. Therefore, no information about the value of k_{OH} is available. The obtained $k_{cat.}$ values are presented in the Supporting Information. The derived sigmoidal pH-rate profiles (Figure 2) are characteristic of a kinetic process controlled by an acid−base equilibrium and exhibit inflection points corresponding to the pK_a values of the coordinated water molecules of **ZnL3** (pK_a = 8.28) and **ZnL8** (pK_a = 7.89). Therefore, the reactive species is concluded to be the Zn(II)−OH^- complex, in which the Zn(II)-bound OH^- acts as a nucleophile to attack intermolecularly the carbonyl group of the acetate ester and hydrolyze thus NA to 4-nitrophenolate and acetate. This mechanism of NA hydrolysis has also been reported for other zinc(II) cyclen complexes.[9,38b]

The k_{NA} values of our zinc(II) cyclen complexes show a 3−4-fold higher hydrolysis rate than the simple Zn[12]aneN$_4$ system due to the aromatic substituent. $\pi-\pi$ interactions of the heterocycle with the aromatic ring of the NA may lead to a tighter binding and provides a more hydrophobic environment[34] with less solvation and therefore a higher reactivity of the hydroxy species. Tang et al. previously reported on the influence of an aromatic substituent, emphasizing its positive influence on the substrate orientation and stabilization of the leaving group in the transition state.[44]

Among the mononuclear Zn complexes, **ZnL8** has the highest hydrolytic activity. Because of its smaller pK_a value, it has a higher percentage of catalytically active species at lower pH values. The lower reaction rate of **ZnL3** may be explained as being due to the bulky azacrown ether in the ortho position.

Several conclusions can be drawn from the comparison of our complexes with previously reported catalysts. First, Zn[12]aneN$_4$ complexes show higher reaction rates than Zn[12]aneN$_3$ derivatives. For the latter complexes, the metal ion is coordinated by only three N atoms; therefore, the electron deficiency of the Zn(II) ion is less saturated, leading to a higher Lewis acidic character of the metal ion but also to a lower nucleophilic character of the Zn−L−OH^- species. The complexes with an ethylhydroxyl pendant arm show a higher hydrolytic activity but operate by a different reaction mechanism, with the alcoholate as the reactive species and a transacylation reaction step. Among the previously reported complexes, Zn[15]aneN$_3$−O$_2$ reported by Bencini et al. has the highest reaction rate (0.6 M^{-1} s^{-1}), comparable to the k_{NA} value of **ZnL8** and **ZnL1** (0.4 M^{-1} s^{-1}). However, these reaction rates are still far from those of natural enzymes, as given in Table 5.

(40) Bazzicalupi, C.; Bencini, A.; Bianchi, A.; Fusi, V.; Giorgi, C.; Paoletti, P.; Valtancoli, B.; Zanchi, D. *Inorg. Chem.* **1997**, *36*, 2784.
(41) Xia, J.; Xu, Y.; Li, S.-A.; Sun, W.-Y.; Yu, K.-B.; Tang, W.-X. *Inorg. Chem.* **2001**, *40*, 2394.
(42) di Targiani, R. C.; Chang, S.; Salter, M. H.; Hancock, R. D.; Goldberg, D. P. *Inorg. Chem.* **2003**, *42*, 5825.
(43) Kiefer, L. L.; Fierke, C. A. *Biochemistry* **1994**, *33*, 15233.
(44) Li, S.-A.; Xia, J.; Yang, D.-X.; Xu, Y.; Li, D.-F.; Wu, M.-F.; Tang, W.-X. *Inorg. Chem.* **2002**, *41*, 1807.

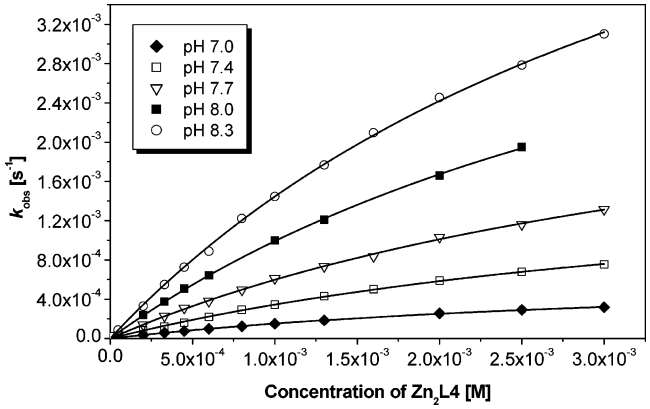

Figure 3. Saturation kinetics for **Zn_2L4** (50 mM Tris/HCl buffer, 10% CH_3CN, I = 0.1 M (NaCl), 25 °C, [NA] = (1.0−4.0) × 10^{-5} M, ΔpH = ±0.01, Δk_{obs} ± 0.5−2.9%).

Because of the chosen reaction conditions, the metal complexes cannot act catalytically. Therefore, an experiment with a catalytic amount of metal complex (the ratio of NA/**ZnL8** is 30:1; [NA] = 0.2 mM; [**ZnL8**] = 0.007 mM) at pH 8 (50 mM Tris/HCl buffer, 25 °C, I = 0.1, NaCl) was performed, and the reaction was followed for 9 h. After this reaction time, a concentration of 0.0107 mM 4-nitrophenolate was recorded, corresponding to a turnover of 151%, thus indicating the catalytic properties of the metal complexes for the hydrolysis of carboxyesters.

Hydrolysis of NA Promoted by the Dinuclear Metal Complexes Zn_2L2, Zn_2L4, and Zn_2L5. The ester bond cleavage rates were measured in a 10% (v/v) CH_3CN aqueous solution in the pH range of 7−8.3 (50 mM Tris/HCl buffer, I = 0.1 M, NaCl) at 25 °C. The concentrations of the complex varied in the range of 0.005−3 mM and those of NA in the range of 0.003−2 mM. In contrast to the mononuclear complexes, here the plots of k_{obs} vs the metal complex concentration at a given pH did not give a straight line but a curve because of saturation kinetics at higher complex concentrations (Figure 3). The plots for the other two complexes are presented in the Supporting Information.

This is typical for a Michaelis−Menten reaction mechanism, where an intermediate substrate/catalyst adduct is formed and then breaks down to release catalyst and reaction products.[45] However, unlike the classical Michaelis−Menten reaction, here the metal complex is the reaction partner present in excess, because of the necessary experimental conditions, also emphasized for other complexes of this type.[16c,24b,36,46] Therefore, the reaction order for the complex concentration is lower than 1. The model for the calculation of the maximum reaction rate $k'_{cat.}$ (s^{-1}), of the apparent association constant for the ester/metal complex/adduct, and of the second-order rate constant $k'_{cat.}/K_M$ (M^{-1} s^{-1}) was established on the basis of previously reported models.[47]

The total rate of reaction v at a constant pH is the sum of the spontaneous hydrolysis and of the metal-catalyzed hydrolysis.[48]

$$v = \frac{d(\text{Abs})}{d(t)\,\epsilon_{obs}} = k'_{obs}([NA] + [Zn_2{-}L{-}NA]) = k_{spontaneous}[NA] + k'_{cat.}[Zn_2{-}L{-}NA] \quad (3)$$

For saturation kinetics, the concentration of the metal complex forming the substrate/catalyst adduct, [Zn_2−L−NA], is the most important. The relationship between this value and the total amount of the metal complex [Zn_2−L] is expressed in eq 4. The K_M and K_A values correspond to the

$$Zn_2{-}L + NA \rightleftharpoons Zn_2{-}L{-}NA \qquad K_A = \frac{[Zn_2{-}L{-}NA]}{[Zn_2{-}L][NA]} \quad \text{with } K_M = K_A^{-1} \quad (4)$$

apparent association constant for the ester/metal complex/adduct.

By extrapolation, we obtain eq 5. By subtraction from the

$$k'_{obs} = \frac{K_M k_{spontaneous} + k'_{cat}\cdot[Zn{-}L]}{K_M + [Zn{-}L]} = \frac{K_M k_{spontaneous}}{K_M + [Zn{-}L]} + \frac{k'_{cat}\cdot[Zn{-}L]}{K_M + [Zn{-}L]} \quad (5)$$

k'_{obs} value, the value of the spontaneous hydrolysis, eq 5 can be written as follows:

$$k_{obs} = \frac{k'_{cat}\cdot[Zn{-}L]}{K_M + [Zn{-}L]} \qquad \text{with: } k_{obs} = k'_{obs} - k_{spontaneous} \quad (6)$$

The curves in Figure 3 were obtained by a nonlinear fit of eq 6. The detailed results derived from these curves are presented in the Supporting Information.

The values of the apparent pH-independent Michaelis−Menten constants K_M are 3.86, 4.34, and 4.2 M for **Zn_2L2**, **Zn_2L4**, and **Zn_2L5**, respectively. From these values, the apparent binding constant K_A for the three complexes can be derived, 0.23 ± 0.02 M^{-1}. The pH-independent k_{NA} values are extrapolated from the second-order reaction rate constants $k_{cat.}$, defined as $k'_{cat.}/K_M$. For these calculations, we assume the monohydroxy species $Zn_2{-}L{-}(OH_2)(OH^-)$ to be the catalytically active species because the dihydroxy form $Zn_2{-}L{-}(OH^-)_2$ is present in a very low concentration for this pH range (at pH 8.3, <3%). Consequently, the values of k_{NA} are 4.1 ± 0.27, 3.1 ± 0.19, and 4.4 ± 0.31 M^{-1} s^{-1} for **Zn_2L2**, **Zn_2L4**, and **Zn_2L5**, respectively. The pK_a value can also be determined kinetically (see also eq 4 in the Supporting Information).[16c] The obtained pK_a values of 8.09 ± 0.17, 8.17 ± 0.16, and 8.37 ± 0.19 for **Zn_2L2**, **Zn_2L4**, and **Zn_2L5**, respectively,[49] correspond within the error margin to the pK_{a1} values determined by potentiometric titrations. Therefore, the

(45) Voet, D.; Voet, J. G. *Biochemistry*, 2nd ed.; Wiley: New York, 1995; p 351.
(46) (a) Gomez-Tagle, P.; Yatsimirsky, A. K. *Inorg. Chem.* **2001**, *40*, 3786. (b) Roigk, A.; Hettich, R.; Schneider, H.-J. *Inorg. Chem.* **1998**, *37*, 751. (c) Hettich, R.; Schneider, H.-J. *J. Am. Chem. Soc.* **1997**, *119*, 5638. (d) Tecilla, P.; Tonellato, U.; Veronese, A. *J. Org. Chem.* **1997**, *62*, 7621.
(47) Kim, D. H.; Lee, S. S. *Bioorg. Med. Chem.* **2000**, *8*, 647.

(48) $k_{spontaneous}$ (s^{-1}) is different for every pH value and does not correspond to the k_{OH} value (M^{-1} s^{-1}). See also eq 7 from the Supporting Information.
(49) For calculation of the pK_a values, the highest error for $k_{cat.}$ is $\Delta k_{cat.}$ ± 8.5%.

Scheme 6. Proposed Associative Reaction Mechanism for the Hydrolysis of Na by **Zn_2L2**, **Zn_2L4**, and **Zn_2L5**

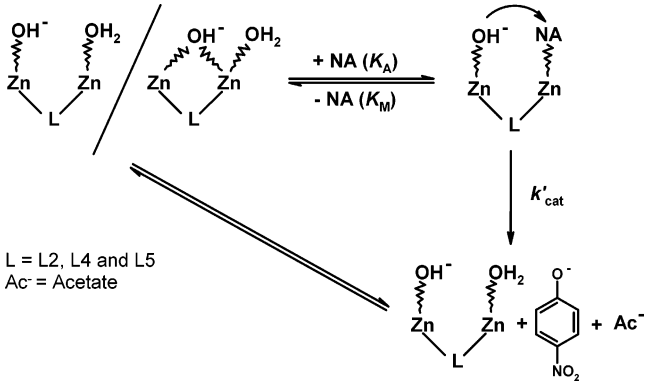

reactive species is in this case the monohydroxy species $Zn_2-L-(OH_2)(OH^-)$ in its open form. The intramolecular reaction mechanism is pictured in Scheme 6.

The monohydroxy species (open and/or closed structure) forms a substrate/catalyst adduct, whereby the ester is displacing a water molecule. Most likely, the ester is coordinating to the metal center through its carbonyl group. The open form is more suitable for coordination of the substrate. Once the hydrolytically relevant species is formed, the intramolecular nucleophilic attack takes place. This attack is facilitated by the additional activation of the ester through its coordination to the metal. A product inhibition study of **Zn_2L2** and **Zn_2L4** with 4-nitrophenolate showed no binding affinity. The same mechanism was reported for the hydrolysis of NA with other Zn(II) complexes of this type.[10c,46,50]

Zn_2L2 and **Zn_2L5** have almost the same catalytic activity, while **Zn_2L4** is about 25% less efficient because of the aforementioned steric factors. The dinuclear complexes are cleaving the ester about 10 times faster than their mononuclear analogues and about 30−44 times faster than the Zn[12]aneN$_4$ complex. This high acceleration rate indicates a cooperation of the two metal centers and supports the proposed mechanism presented in Scheme 6.

Hydrolysis of NA Promoted by the Dinuclear Metal Complexes Cu_2L2, Ni_2L2, Zn_2L6, and Zn_2L7. The ester bond cleavage rates were measured in a 10% (v/v) CH_3CN aqueous solution in the pH range of 6−9.5 (50 mM Tris/HCl, HEPES, or CHES buffer, $I = 0.1$ M, NaCl) at 25 °C under pseudo-first-order reaction rate conditions (excess of the metal complex).

The reaction rate is proportional to the concentrations of the metal complex and the substrate, such that eq 7 can be postulated, from which eq 8 is then easily derived. The

$$v_{cat.} = k_{cat.}[Zn-L]^{Total}[NA] \quad (7)$$

$$v_{cat.} = \frac{d(Abs)}{d(t)\,\epsilon_{obs}} = k_{obs\ 1,2}[NA] = k_{cat.\ 1,2}[Zn-L]^{Total}[NA] \quad (8)$$

reaction rate $v_{cat.}$ reflects in this case the contribution of two reactive species, the monohydroxy and dihydroxy species. Therefore, eq 8 can be interpolated to eq 9.

$$k_{cat.\ 1,2}[Zn-L]^{Total} = k_{cat.\ 1}[Zn_2-L-(OH_2)(OH^-)] + k_{cat.2}[Zn_2-L-(OH^-)_2] \quad (9)$$

For **Ni_2L2**, low hydrolysis rates (k_{obs} in the range of 10^{-6} s^{-1}) were obtained because of the weak Lewis acidic character of the metal ion reflected in the high pK_a values of the complex (9.74 and 10.13). Therefore, at physiological pH, there is no active species present in solution. For measurement with this complex, as well as with **Cu_2L2**, difficulties were encountered when measuring the hydrolysis rates under the chosen reaction conditions. The concentration range needed for these complexes in order to have a stable baseline and acceptable experimental errors required low concentrations of the metal complex, which led to low concentrations of the substrate in order to have $C_0 \gg S_0$, reaching the detection limits of the apparatus. Together with long induction periods for **Cu_2L2**, for which we do not yet have a rational explanation, the kinetic measurements remain difficult to interpret. To the best of our knowledge, no copper(II) or nickel(II) cyclen complexes promoting the hydrolysis of a carboxyester are reported, while phosphate ester hydrolysis was reported for Cu[9]aneN$_3$ complexes[51] and Ni(II) complexes.[23] However, a successful carboxyester hydrolysis promoted by **Ni_2L2** is clearly not possible in the pH range of 7−9 because of the low Lewis acidity of the metal and most improbable for the **Cu_2L2** complex because of the fact that the two metal centers do not act cooperatively (as indicated by the small difference between the two pK_a values) and that each Cu(II) cation has only one available coordination site, making it impossible to bind both substrate and hydroxide on the same metal ion. Morrow et al.[52] and Hegg and Burstyn[14a] have demonstrated that artificial metallohydrolases (mononuclear as well as dinuclear metal complexes) must possess two cis-oriented labile coordination sites in order to bind both substrate and nucleophile, which is not the case for **Cu_2L2**.

For **Zn_2L7**, the difference between its pK_a values is too small to allow a separate study of the influence of the monohydroxy and dihydroxy species, as for **Zn_2L6** or for previously reported compounds.[24a,37,43,53] From the plots of $k_{obs1,2}$ vs the metal complex concentration at a given pH, the $k_{cat.\ 1,2}$ values for **Zn_2L7** were obtained (Table 11 of the Supporting Information). The pH−rate profile is presented in Figure 4. For pH <6, no hydrolytic activity is measurable; therefore, both species are active species. For pH >10, only the dihydroxy species $Zn_2-L-(OH^-)_2$ is present in solution; hence, $k_{cat.\ 1,2}$ is in this case equal to $k_{cat.\ 2}$.

From the species distribution diagram and the experimentally determined $k_{cat.\ 1,2}$ values, it is possible to derive the

(50) (a) Breslow, R.; Singh, S. *Bioorg. Chem.* **1988**, *16*, 408. (b) Breslow, R.; Nesnas, N. *Tetrahedron Lett.* **1999**, *40*, 3335. (c) Akkaya, E. U.; Czarnik, A. W. *J. Am. Chem. Soc.* **1988**, *110*, 8553.

(51) Fry, F. H.; Fischmann, A. J.; Belousoff, M. J.; Spiccia, L.; Brügger, J. *Inorg. Chem.* **2005**, *44*, 941 and references cited therein.

(52) Iranzo, O.; Richard, J. P.; Morrow, J. P. *Inorg. Chem.* **2004**, *43*, 1743.

(53) Xia, J.; Li, S.-A.; Shi, Y.-B.; Yu, K.-B.; Tang, W.-X. *J. Chem. Soc., Dalton Trans.* **2001**, 2109.

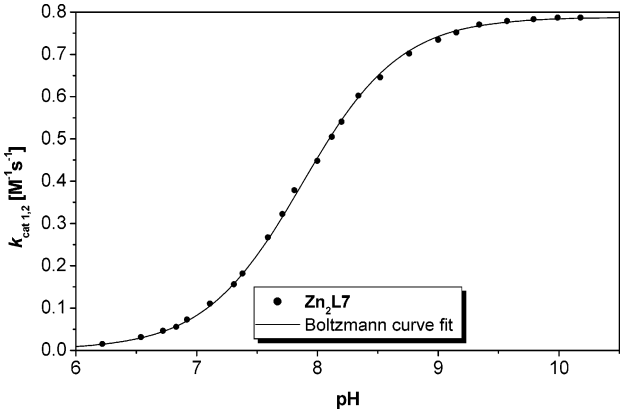

Figure 4. pH−rate profile for the second-order rate constants of NA hydrolysis of **Zn$_2$L7** at 25 °C and I = 0.10 (NaCl) in 10% (v/v) CH_3CN.

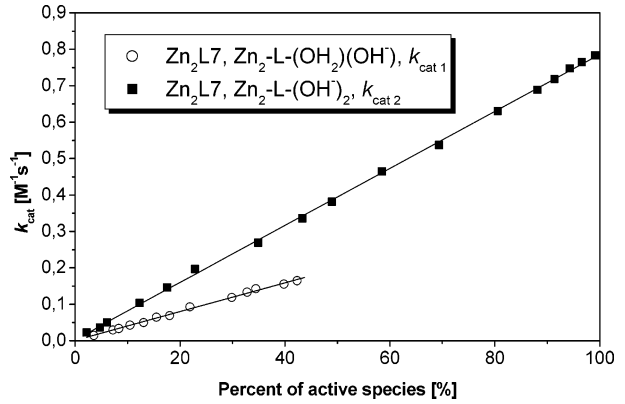

Figure 5. Deduction of $k_{cat.\,1}$ and $k_{cat.\,2}$ from the values of $k_{cat.\,1,2}$ for **Zn$_2$L7**.

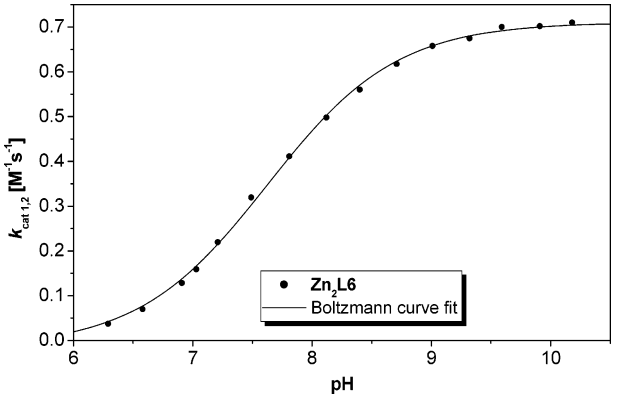

Figure 6. pH−rate profile for the second-order rate constants of NA hydrolysis of **Zn$_2$L6** at 25 °C and I = 0.10 (NaCl) in 10% (v/v) CH_3CN.

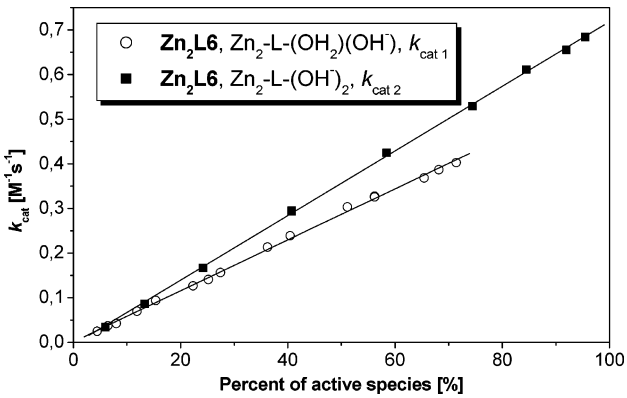

Figure 7. Deduction of $k_{cat.\,1}$ and $k_{cat.\,2}$ from the values of $k_{cat.\,1,2}$ for **Zn$_2$L6**.

values of $k_{cat.\,1}$ and $k_{cat.\,2}$ from calculations[54] (Figure 5; for more details, see Figures 24 and 25 of the Supporting Information).

Once the pH-dependent $k_{cat.\,1}$ and $k_{cat.\,2}$ values are known, the k_{NA} values can be easily derived. The values of $k_{NA\,1}$ and $k_{NA\,2}$ for **Zn$_2$L7**, corresponding to the monohydroxy species $Zn_2-L-(OH_2)(OH^-)$ and the dihydroxy species $Zn_2-L-(OH^-)_2$, respectively, are 0.40 ± 0.007 and 0.78 ± 0.006 M^{-1} s^{-1}, respectively. A comparison of these values with those of the mononuclear complexes shows that the k_{NA} values of **ZnL1** and **ZnL8** are almost identical with the $k_{NA\,1}$ value and that the value of $k_{NA\,2}$ is 2 times higher than that of the mononuclear complexes. Hence, it seems that for **Zn$_2$L7** the two metal centers are acting independently in the hydrolysis of 4-nitrophenyl acetate.

The same calculations based on eq 8 were performed for **Zn$_2$L6**. The pH−rate profile (Figure 6) has a sigmoidal shape, with the velocity of the reaction tending to zero for lower pH values and reaching a maximum for high pH values.

The pK_a values of **Zn$_2$L6** are more differentiated, permitting thus a better separation of the two reactive species and of their second-order reaction rate constants $k_{cat.\,1}$ and $k_{cat.\,2}$. For pH values of below 7, the amount of dihydroxy species present in solution is less than 0.5%; hence, the $k_{cat.\,1,2}$ value corresponds in this range to the $k_{cat.\,1}$ value. For the remaining pH range, we used the same calculation method as that for **Zn$_2$L7** (Figure 7).

The values of $k_{NA\,1}$ and $k_{NA\,2}$ for **Zn$_2$L6** are 0.57 ± 0.003 and 0.72 ± 0.004 M^{-1} s^{-1}, respectively. A comparison of the reaction rates of **Zn$_2$L6**, **Zn$_2$L7**, and **ZnL8** shows the monohydroxy species of **Zn$_2$L6** possessing a 45% higher rate than the others, whereas the monohydroxy species of **Zn$_2$L7** is in the same range as that of **ZnL8**. Moreover, the rate of the dihydroxy species of **Zn$_2$L6** is about 10% lower than the rate of **Zn$_2$L7**. These facts indicate a different behavior of the metal centers. Actually, the mechanism of hydrolysis for **Zn$_2$L6** seems to be a hybrid between the one postulated for the aryl-bridged **Zn$_2$L5** (cooperation of the metal centers and intramolecular nucleophilic attack) and the one established for the triaryl-bridged **Zn$_2$L7** (independence of the metal centers and intermolecular nucleophlic attack). Indeed, the experimental data for the diaryl-bridged **Zn$_2$L6** could also be fitted to the saturation kinetics model with similar regression coefficients.[55] We conclude that the mechanism of the reaction is defined by the degree of

(54) Bazzicalupi, C.; Bencini, A.; Berni, E.; Giorgi, C.; Maoggi, S.; Valtancoli, B. *J. Chem. Soc., Dalton Trans.* **2003**, 3574.

(55) Interpretation of the experimental data at pH 7 using eq 6: $k'_{cat.}$ = $2.14 \times 10^{-3} \pm 8.0 \times 10^{-5}$ s^{-1}; $K_M = 1.36 \times 10^{-2} \pm 5.3 \times 10^{-4}$ M; $k_{cat.} = k'_{cat.}/K_M = 0.157$ M^{-1} s^{-1}; $K_A = 74$ M^{-1} ($R^2 = 0.9998$).

(56) Bencini, A.; Berni, E.; Bianchi, A.; Fedi, V.; Giorgi, C.; Paoletti, P.; Valtancoli, B. *Inorg. Chem.* **1999**, *38*, 6323.

Table 7. Comparison of Hydrolysis Rate Constants k_{NA} (M^{-1} s^{-1}) and pK_a Values for Previously Reported Di- and Trinuclear Zn(II) Metal Complexes

complex/nucleophile	$10^2 k_{NA}$ (M^{-1} s^{-1})[a]	pK_a[b]	lit.
Zn_2[30]aneN_6O_4/Zn_2−OH^-	9.4 ± 0.1	7.6	39
Zn_2[30]aneN_6O_4/Zn_2−$(OH^-)_2$	130 ± 10	9.2	39
Zn_2[30]aneN_6O_4−ethyl−OH/Zn_2−(ethyl−OH^-)	21 ± 2	6.9	37
Zn_2[30]aneN_6O_4−ethyl−OH/Zn_2−(ethyl−OH^-)(OH^-)	160 ± 10	8.5	37
Zn_2[36]aneN_8O_4/Zn_2−OH^-	35 ± 4	7.9	56
Zn_2[36]aneN_8O_4/Zn_2−$(OH^-)_2$	350 ± 30	9.4	53
Zn_2[33]aneN_7O_4/Zn_2−OH^-	16 ± 2	7.5	53
Zn_2[33]aneN_7O_4/Zn_2−$(OH^-)_2$	200 ± 20	9.1	53
Zn_3−Tren−([14]aneN_4))$_3$/Zn_3−$(OH^-)_2$[c]	34 ± 4	8.1	51
Zn_3−Tren−([14]aneN_4))$_3$/Zn_3−$(OH^-)_3$	370 ± 40	8.9	51
Zn_3−Tren−([12]aneN_4))$_3$/Zn_3−$(OH^-)_2$[c]	56 ± 6	8.6	51
Zn_3−Tren−([12]aneN_4))$_3$/Zn_3−$(OH^-)_3$	420 ± 40	9.7	51

[a] Various buffer systems [50 mM], 10% CH_3CN, I = 0.1−0.15 M (NaCl or NMe_4NO_3), 25 °C. [b] 25 °C, water, the first decimal was rounded up. [c] pK_a and k_{NA} values of the monohydroxy species were not determined because of their negligible effect on the hydrolysis.

Chart 4. Structures of Previously Studied Di- and Trinuclear Zn(II) Complexes for the Hydrolysis of NA[a]

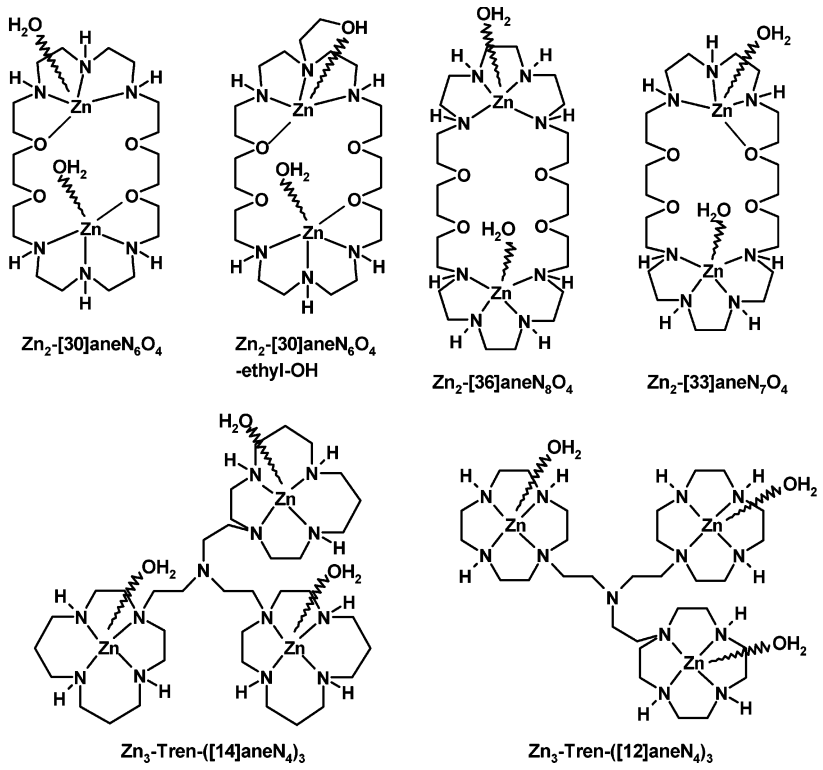

[a] Charges and counterions are omitted for clarity reasons.

cooperation between the metal centers, influenced by the spacer length.

The structures of the most efficient previously reported di- and trinuclear metal complexes are depicted in Chart 4, and their reported second-order reaction rates k_{NA} and pK_a values are presented in Table 7.

For all of the reported complexes, a bimolecular mechanism is postulated, with the coordinated hydroxide acting as the nucleophile. For the complexes with a pendant arm, another mechanism is valid and has already been described for the mononuclear complexes. The metal centers in these complexes are not rigidly bound, as is the case for the compounds reported here. This leads to much lower hydrolysis rates of the monohydroxy species compared to the dihydroxy species because of intramolecular folding leading to steric hindrance. Hence, a rigid structure is advantageous for the hydrolytic efficiency of the complex.

The monohydroxy species of **Zn_2L6** and **Zn_2L7** hydrolyze NA 1.5−5.5 times faster than the complexes in Table 7, while **Zn_2L2**, **Zn_2L4**, and **Zn_2L5** are about in the same range as the Zn_3−Tren−([12]aneN_4))$_3$ complex. Overall, our complexes are in the same range as previously reported similar compounds but have a higher hydrolytic activity at physiological pH values (e.g., **Zn_2L2** has, at pH 8.3, $k_{cat.}$ = >2 M^{-1} s^{-1}, a value which for Zn_3−Tren−([12]aneN_4))$_3$ is reached only at pH >10).[51] Therefore, the complexes reported in this paper are better suited for the hydrolysis of esters under physiological conditions.

The catalytic property of all dinuclear Zn(II) complexes was tested by performing experiments with an excess amount of NA ([NA] = 1−2 mM; [metal complex] = 0.005−0.01 mM) in the pH range of 6.7−7.1 (50 mM HEPES buffer, 25 °C, I = 0.1, NaCl) and following the reaction for longer time periods. The turnovers of NA are 3.9 times higher than

Table 8. Summary of the Hydrolytic Assays for NA

complex/nucleophile	$10^2 k_{NA}$ (M^{-1} s^{-1})	pK_a
zinc cyclen	9.6 ± 0.01	7.9
ZnL1; $Zn_1L(OH^-)$	39.1 ± 0.1	8.35
ZnL3; $Zn_1L(OH^-)$	27.9 ± 0.01	8.28
ZnL8; $Zn_1L(OH^-)$	38.6 ± 0.02	7.89
Zn_2L2; $Zn_2L(OH^-)(OH_2)$	410 ± 27	8.09[a]
Zn_2L4; $Zn_2L(OH^-)(OH_2)$	310 ± 19	8.27
Zn_2L5; $Zn_2L(OH^-)(OH_2)$	440 ± 31	8.37,[a] 8.14[b]
Zn_2L6; $Zn_2L(OH^-)(OH_2)$	57.3 ± 0.3	7.45
Zn_2L6; $Zn_2L(OH^-)(OH^-)$	71.7 ± 0.4	8.85
Zn_2L7; $Zn_2L(OH^-)(OH_2)$	39.9 ± 0.74	7.65
Zn_2L7; $Zn_2L(OH^-)(OH^-)$	78.6 ± 0.6	8.11

[a] Determined kinetically. [b] MeOH/H_2O (9:1).

the complex concentrations, thus indicating the catalytic properties of the metal complexes for the hydrolysis of carboxyesters.[57]

Conclusion

All determined k_{NA} and pK_a values of the active species of the mono- and dinuclear metal complexes are summarized in Table 8.

The k_{NA} values of the mononuclear zinc(II) cyclen complexes show a 3−4-fold higher hydrolysis rate than the simple Zn[12]aneN_4 system because of the aromatic substituent, which provides a more hydrophobic environment[34] and interacts with the aromatic ring of the NA by $\pi-\pi$ interactions. The reactive species is the Zn(II)−OH^- complex, in which the Zn(II)-bound OH^- acts as a nucleophile to attack intermolecularly the carbonyl group of the acetate ester.

For the dinuclear complexes, the mechanism of the reaction is defined by the degree of cooperation between the metal centers, influenced by the spacer length. The spacer type does not have an important influence on the catalytic activity, as can be observed from the similar k_{NA} values of **Zn_2L2** and **Zn_2L5**. For **Zn_2L7**, possessing the longest spacer, the two metal centers act independently in the hydrolysis; therefore, the reaction rate is twice as high as the rate of the mononuclear analogue. The complexes with one aryl spacer show saturation kinetics with formation of a Michaelis−Menten adduct. Their rates are 40 times higher than the simple Zn[12]aneN_4 system. **Zn_2L6** is a hybrid between these two mechanisms; a clear saturation curve is not visible, nor are the metal cores completely independent from another.

The Cu(II) and Ni(II) complexes do not fulfill one of the two conditions needed for an artificial metallohydrolase: the Cu(II) complexes do not possess two cis-oriented coordination sites on the metal ion for binding of the substrate and a water molecule, while Ni(II) is not a strong Lewis acid in **NiL1** and **Ni_2L2** and does not facilitate deprotonation of the coordinated water to generate the hydroxide nucleophile.

For all Zn(II) complexes, the catalytic activity was proven. The Zn(II) complexes show a higher concentration of active species under physiological conditions than previously reported similar compounds and are therefore well suited for the hydrolysis of esters under physiological conditions.

Acknowledgment. The authors thank Schering AG, Berlin, for providing the cyclen and the Fond of the Chemical Industry for support. K.W. thanks the Deutsche Bundesstiftung Umwelt for a graduate scholarship.

Supporting Information Available: Crystal data and data collection parameters, atomic positional parameters, bond length, bond angles, torsion angles, and hydrogen bonds of [**Zn_2L2**]μ-OH-$(ClO_4)_3 \cdot CH_3CN \cdot H_2O$, calculation of the molar extinction coefficients for *p*-nitrophenolate, calculation of the spontaneous hydrolysis of NA, pH profiles and species distribution diagrams of all metal complexes, saturation kinetics data for the Zn(II) complexes, second-order rate constants $k_{cat.\ 1,2}$ (M^{-1} s^{-1}) for **Zn_2L6** and **Zn_2L7** and the graphical representation of the relationship between measured $k_{cat.\ 1,2}$, the species distribution diagram, and the calculated $k_{cat.\ 1}$ and $k_{cat.\ 2}$ for **Zn_2L6** and **Zn_2L7**. This material is available free of charge via the Internet at http://pubs.acs.org.

IC070101Z

(57) The hydrolysis rate was not measured by a "log-plot" method. The measured absorption is corrected with the molar extinction coefficient ϵ_{NP} using eq 4 from the Supporting Information and then compared to the complex concentration. Correction for the spontaneous hydrolysis of the substrate by the solvent was accomplished by directly measuring a difference between the production of 4-nitrophenolate in the reaction cell and a reference cell containing the same concentration of carboxyester as that in the reaction cell in the absence of the metal complex.